ACCURACY AND PRECISION OF PERPENDICULAR DISTANCE MEASUREMENTS IN SHIPBOARD LINE-TRANSECT SIGHTING SURVEYS

Douglas Kinzey, Tim Gerrodette and Daniel Fink

Southwest Fisheries Science Center
National Marine Fisheries Service, NOAA
8604 La Jolla Shores Drive
La Jolla, California 92037

JUNE 2002

ADMINISTRATIVE REPORT LJ-02-09

ABSTRACT

The accuracy and precision of two key field measurements used to produce estimates of marine mammal abundance from shipboard surveys – the horizontal angles from the ship's trackline and the radial distances to the animals in the water – were assessed. Measurements were made from two ships, the *McArthur* and the *David Starr Jordan*, under field conditions. Horizontal angles were measured using angle rings and radial distances were measured with reticles in 25X binoculars. Distances to targets were measured simultaneously using radar and reticles. Rounding of horizontal angles in field survey data to 5 degree increments, and of reticle values to both 0.2 and 0.5 reticle increments, was indicated by autocorrelation tests. The rounding was eliminated by "smearing" the original horizontal angles over ± 2 degrees and the original reticles over ± 0.05 reticles. Replicated measurements of angles in the radar database indicated 95% of angle measurements to a single target were expected to be within ± 3 degrees of one another. The precision of radial distances measured using reticles was inversely proportional to target distance. The radial distances calculated using the formula proposed by Lerczak and Hobbs (1998) were a closer fit to distances from radar than alternative formulas, but exhibited a slight tendency to underestimate distances to targets close to the horizon under field conditions. Adjusting reticle measurements for light refraction improved the fit to target distances by reducing this downward bias. A second adjustment corrected ship-specific responses to sea conditions at the time the reticles were used.

INTRODUCTION

The perpendicular distances to marine mammals from a ship's trackline can be used to estimate the mammals' density and abundance using line-transect methods (Buckland et al., 2001; Thomas et al., 1998). On ship surveys conducted by the Southwest Fisheries Science Center (SWFSC), two angular measurements are recorded, the horizontal angle between a mammal sighting and the trackline, and the vertical angle between the sighting and the horizon. The vertical angle is converted to a radial distance using a formula based on spherical geometry (Lerczak and Hobbs, 1998). The perpendicular distance is calculated by multiplying the radial distance by the sine of the horizontal angle.

Biases in recording horizontal angles and radial distances can affect the distribution of perpendicular sighting frequencies, and hence the final estimates of density and abundance (Butterworth, 1982; Hammond, 1984). Barlow and Lee (1994) found evidence of rounding of horizontal angles by observers on surveys conducted prior to 1991 by the SWFSC. Butterworth (1982) developed an analytical "smearing" technique that added randomized terms to the original angle and distance measurements to improve the final estimates when the original measurements had been rounded in the field. Here we examine SWFSC survey data collected during 1998-2000, and a separate database of binocular versus radar measurements of distance at sea, for evidence of bias or inaccuracies in our field measurements. We compare alternative equations for calculating radial distance from binocular reticles and introduce: 1) a method using

autocorrelation to evaluate the sufficiency of data smearing; 2) minor corrections for the effects of refraction on distance measurements near the horizon using reticles or other angle-based devices; and 3) a final correction for ship-specific differences in distances obtained using reticles in 25X binoculars under field survey conditions.

An independent scientific peer review of this work was administered by the Center for Independent Experts located at the university of Miami. Responses to reviewers' comments can be found in Appendix A.

METHODS

Three potential types of error in the calculations of perpendicular sighting distances were examined: rounding of horizontal angles, rounding of reticles, and absolute differences between binocular and radar measurements of radial distance. These provided empirical estimates of the precision and accuracy of radial sighting distances and of the precision of horizontal angle measurements. The accuracy of horizontal angle ring measurements apart from rounding was not explicitly examined in this study.

The horizontal angle was typically measured using an angle ring marked to 1-degree increments at the base of a binocular mounted on a pedestal. The angle ring was calibrated with an alidade on the ship's gyrocompass repeater. A pointer on the ring indicated the bearing to sightings relative to the ship's heading. The vertical angle was measured using a reticle scale in the binocular eyepiece.

Two sources of data were used. The first was a series of field surveys of marine mammal populations in the eastern tropical Pacific Ocean during 1998 to 2000 that produced 4,307 on-effort sightings suitable for line-transect analysis (Kinzey et al., 1999; 2000; 2001). Only sightings made forward of the ship's beam (between trackline angle 0 and 90 degrees left or right) were classified as on-effort during these surveys.

A second source of data was 1,606 paired measurements of the distances to targets from two ships using both radar and the reticles in 25X binoculars under a variety of sighting conditions. These measurements were recorded by the mammal observers during testing periods on shipboard surveys from 1990 to 1993. Most observers were tested on both ships. The target was generally the waterline of a small boat with a radar target set out for the purpose, but occasionally buoys or other floating objects visible to radar were used. Air temperatures, air pressures, and swell heights associated with the measurements were copied from the ship deck logs. Beaufort sea state and a motion code (upswell, downswell, trough) were additionally recorded.

Horizontal Angles

Most of the horizontal sighting angles on the field surveys were measured using angle rings on 25X binoculars (Table 1). Some sightings, however, were made using unaided eye or 7X binoculars and did not include angle ring measurements. The 25X and

non-25X datasets were evaluated separately for angle rounding effects by the following procedure.

Frequency histograms of the sighting angles in 1-degree bins were produced, with equal angles left or right of the trackline combined into a single bin. Preliminary examination of these histograms indicated rounding spikes at 5-degree intervals. We used statistical tests of the difference between autocorrelation coefficients (Zar, 1984) in the angle frequencies to assess the degree of rounding at 5-degree lags versus lags 1 through 9, testing one lag at a time. The test statistic, Z', expected to be normally distributed, was calculated as:

$$Z' = \frac{\ln[(1+r_1)/(1-r_1)] - \ln[(1+r_2)/(1-r_2)]}{2 * \sqrt{1/(n_1-3) + 1/(n_2-3)}}, \quad (1)$$

where
r_1 = autocorrelation coefficient at lag to be tested against 5 degree lag,
r_2 = autocorrelation coefficient at 5 degree lag,
n_1 = number of angles used to calculate r_1, and
n_2 = number of angles used to calculate r_2.

Z' was compared to the normal distribution in a one-tailed test of the null hypothesis that the correlation coefficient of the 5-degree lags was not greater than the coefficient for the tested lag. A significant Z' value indicated that the autocorrelation at the 5 degree lag was greater than the tested lag and therefore rounding was present. The test was applied separately for each value of lag.

The sighting angles were then smeared over several ranges following the method of Butterworth (1982). For each sighting a smeared angle, S_ρ, was calculated as:

$$S_\rho = | \rho + \upsilon \Delta\rho |, \quad (2)$$

where
ρ = original angle recorded in the field,
υ = a uniform random number between -0.5 and 0.5, and
$\Delta\rho$ = the range of angles to be smeared over.

Absolute values of $\rho + \upsilon \Delta\rho$ were used to prevent negative angles as a result of smearing near the trackline.

The frequencies of angles produced by Eq. *2* were tested for rounding effects using Eq. *1*. The statistics in Eq. *1* were calculated from mean values of 20 runs of Eq. *2* applied to each sighting angle. In each run the smeared angle, S_ρ, was rounded to the nearest integer value before calculating the frequency distribution.

Equation *2* randomly distributes a portion of the original angles, dependent on $\Delta\rho$, into adjacent frequencies ± 1/2 $\Delta\rho$ from the original angle. Thus the outermost bins for each level of smearing received only half as many redistributed angles as did the inner

bins. Some smeared 90 degree angles were redistributed to angles greater than 90 degrees, making the sightings off-effort (not to be used in estimating abundance) by our field criteria. This reduction in the original data is reasonable assuming that a final spike at 90 degrees in the field data indicates observers rounded some angles into the on-effort zone that should have been recorded as off-effort.

For the 25X measurements, $\Delta\rho$ values tested were 2, 3, 4, 5, 10, and 15 degrees (±1, ±1.5, ±2, ±2.5, ±5 and ± 7.5 degrees to either side of the original angle, respectively). The non-25X measurements were smeared over these ranges, and also over ±10 and ±15 degrees.

The radar database was used to assess the precision of horizontal angle measurements by comparing the angles assigned by observers in replicated measurements of a single target. A total of 1572 individual angle measurements were made to 517 targets, of which 467 targets were measured three or more times simultaneously by different observers (Table 2). The mean of the 467 standard deviations of these replicated measurements represented the variability in using horizontal angle rings.

Vertical Angles

Radial distances on the field surveys were typically measured with reticles in 25X binoculars (Table 1). Each reticle in the 25X binoculars used by the SWFSC spans 0.0771 degrees (0.00135 radians; Kinzey and Gerrodette, 2001). The scale is marked to every 0.2 reticles between 0 and 2 reticles and to every half reticle from 2 to 20. Reading reticle values to the inscribed precision would thus result in two levels of rounding, one at every 0.2 reticles for measurements less than two reticles and the other at every 0.5 reticles for measurements greater than two reticles.

The effect of rounding reticles on distance measurement is most pronounced at small reticle values near the horizon. Observers are instructed to record the more distant sightings, those made at less than 2 reticles, to the nearest 0.1 reticle. The distance between an object located at 0.1 reticle and one at 0.2 reticles from a 10.7 m platform is 1.1 km (0.6 nm). By comparison, the difference between 2.0 and 2.1 reticles is less than 0.1 km and between 20 and 20.1 reticles the difference is less than 2 m.

Rounding of reticles was evaluated similarly to the rounding of horizontal angles. Reticle frequencies from the 1998-2000 surveys were binned at 0.1 reticle intervals. Two potential levels of rounding, at every 0.2 reticles for measurements ≤ 2 reticles, and at every 0.5 reticles for all reticle measurements, were tested against lags 0.1 to 0.9. Tests of the correlation coefficients of spikes in the field data using Eq. 1 were performed. The data were then smeared using Eq. 2 and the results retested.

Converting Reticle Values to Distances

Lerczak and Hobbs (1998) provide exact theoretical formulas for converting vertical angles to radial distances. Alternative formulas that give equal numerical results

are given in Gordon (1990), Jaramillo et al. (1999) and Buckland et al. (2001). The formulas require two angle terms when binocular reticles are used as the measuring device. The angle from the horizon down to the target (θ in Lerczak-Hobbs formulation) is measured using reticles, and a second angle (α) above the horizon to the horizontal tangent is calculated from observer height. For brevity, we will refer to θ as the target angle and to α as the above-horizon angle. Both angles, in radians, are summed to calculate distance, D_{LH}, to the target in kilometers as follows:

$$D_{\mathrm{LH}} = h_e * \sin(\theta + \alpha) - \sqrt{R_E^2 - (h_e * \cos(\theta + \alpha))^2}\ , \qquad (3)$$

where
θ = angle below the horizon, in radians,
α = angle from horizontal tangent to horizon = $\mathrm{atan}(\sqrt{2R_E h + h^2}\ / R_E)$,
h = eye height above sea level, in km,
R_E = radius of earth (= 6371 km),
$h_e = R_E + h$.

The distance to the horizon is given by the square root term ($\sqrt{2R_E h + h^2}$) in the definition of α.

Target distances in the radar database ranged between 0.33 and 10.35 km (the horizon was approximately 11.6 km). In addition to Eq. *3*, we tested several other formulas for converting vertical angles to distances that produce different numerical results. These are given in Smith (1982), Buckland et al. (1993), and Bowditch (1995) (Table 3). Reticles below the horizon for each target were converted to distances using the various formulas and plotted against the distances measured with radar.

Once the best distance formula was identified, a number of adjustments or modifications to reduce bias were explored. The improvements achieved using the adjusted distances were compared visually by plotting and statistically by using minimum mean squared errors or, for the final adjustments, the small-sample version of Akaike's Information Criterion ($\mathrm{AIC_c}$; Burnham and Anderson, 1998).

The precision of 25X measurements of radial distance was assessed in two ways, one that included bias (accuracy) and one that did not (measurement error). Variance of the distances from reticles increased with target distance, suggesting errors were multiplicative rather than additive. An approximate 95% confidence interval for a given distance, *D*, was *D*/*P* for the lower and *D***P* for the upper bounds, where

$$P = \exp(1.96 * \sigma), \qquad (4)$$

and σ = standard deviation of the logarithm of distance, estimated as described below.

One estimate of σ in Eq. *4* was similar to the method used in determining precision for horizontal angles. Three or more reticle measurements were made to 502

separate targets (Table 2). This first estimate of σ was the mean of the 502 standard deviations of the logarithms of distances from reticles to a single target, s_1, where:

$$s_1 = \sum_{i=1}^{502} \left[\frac{n\sum_j d_{\mathrm{LH},j}{}^2 - (\sum_j d_{\mathrm{LH},j})^2}{n(n-1)} \right]^{1/2} / 502 , \qquad (5)$$

with
n = the number of repeated measurements (3 - 6) to a single target, and
$d_{\mathrm{LH},j} = ln(D_{\mathrm{LH}})$ for the jth observation, j = 1, . . ., n.

This calculation of precision indicates the variability of repeated measurements to a target, but not any systematic bias that would cause the mean of those measurements to differ from the true distance. s_1 will overestimate precision to the extent that systematic errors result in E(D_{LH}) not equaling D. It represents the maximum precision potentially attainable using unbiased reticle measurements, given the variability observed in simultaneous, replicated measurements under field conditions.

The second method of calculating σ incorporated bias as well as variability. In this method, σ in Eq. *4* was represented by the root mean squared error between logarithms of distances from reticles and radar, s_2, where:

$$s_2(\text{including bias}) = \sqrt{\frac{\sum (d_{2,k} - d_k)^2}{m}} , \qquad (6)$$

and
m = total number of paired reticle and radar measurements,
$d_{2,k}$ = logarithm of distance from reticles (d_{LH} or its adjusted values, see below) for the k^{th} measurement, k = 1, . . ., m, and
d_k = logarithm of distance from radar for the k^{th} measurement.

Confidence intervals based on the method of estimating σ by Eq. *6* were wider than those using Eq. 5. The difference between the two is an indication of the amount of total variability in reticle measurements that could be due to a biased rather than random component.

Correcting Distances Based on Refraction

Equation *3* assumes that light travels in straight lines. It does not account for possible bending due to environmental conditions that can cause refraction (Lerczak and Hobbs, 1998). However, light rays curve when passing obliquely through an atmospheric density gradient (Fleagle and Businger, 1980; Leaper and Gordon, 2001). Atmospheric density typically decreases with height, which results in a decrease in the perceived vertical angle between a distant object at sea level and the horizontal tangent when the light arrives at an observer. The object is perceived higher relative to the observer than it

is based on geometry. This refraction effect is greatest at the horizon, so that although both horizon and target angles from the horizontal tangent decrease as a result of refraction, the *relative* angle between the object and the horizon *increases*. These combined effects on the target and horizon angles result in underestimation of the object's distance when a geometry-based formula such as Eq. *3* is used.

The eye heights on the two ships used for the field surveys and the radar measurements were 10.4 m above the water for the *McArthur* and 10.7 m for the *David Starr Jordan*. On field surveys, the initial sightings to mammal schools are made as far from the ship as possible, resulting in very small sighting angles near the horizon. For an object at 0.1 reticle this angle, θ (Eq. *3*), is 0.000135 radians (0.0077 degrees). The above-horizon angle (α) for a 10.4 m high platform is 0.00181 radians (0.1037 degrees). Although Eq. 3 is the most geometrically accurate formula for angles of this small magnitude (Buckland et al., 2001), these near-horizon angles are also those for which refraction effects are expected to be greatest (Leaper and Gordon, 2001).

Adjusting α only: Two methods incorporating the effects of refraction on reticle measurements were compared. The first was based on a correction to the above-horizon angle in Eq. *3*, sometimes called the "dip of the visible horizon", based on average refraction effects. Bowditch (1995) provides an empirically based correction for α that accounts for the average effect of refraction on the dip of the visible horizon at sea. This standard correction, α_B, in radians, is:

$$\alpha_B = 1.76\sqrt{h_m}\,\frac{\pi}{1080}, \qquad (7)$$

where
h_m = observer height in meters above sea level.

The $\pi/1080$ term converts Bowditch's original value in minutes of arc to radians. The angle of dip calculated from Eq. *7* is about 91% of the α value in Eq. *3*. For a platform height of 10.4 m, this standard correction had the effect of raising the perceived horizon from 0.00181 to 0.00165 radians, or by a little more than 0.1 reticle. The target angle, θ, was unmodified in this method.

Adjusting both α and θ*:* The second method of correcting Eq. *3* for refraction used air temperature, air pressure, and air temperature gradient to adjust both the above-horizon and target angles. Air temperatures and pressures were recorded at the time the reticle *vs* radar measurements were made. Leaper and Gordon (2001) provide formulas for calculating refraction directly from these environmental data when the measurements are taken for objects at known distance from the observer. The method involves calculating the radius of the arc of the refracted ray of light, which is then used in calculating the angle of dip and the angle below the horizon. The first empirical term is atmospheric density, A (kg/m^3):

$$A = \frac{p\beta}{T}, \qquad (8)$$

where
p = atmospheric pressure in Pa (= 100 X mb = kg m^{-1} s^{-2}),
T = air temperature in degrees Kelvin,
β = reciprocal of specific gas constant = 0.00348 m^{-2} s^2 degrees[1].

Atmospheric density is then combined with the temperature gradient to calculate a "radius of curvature", r, of the refracted ray in meters:

$$\frac{1}{r} = \frac{\varepsilon A}{(1+\varepsilon A)T}\left(\frac{\Delta T}{\Delta h} + g\beta\right), \tag{9}$$

where
ε = (refractive index of air - 1)/ standard density at sea level = 0.000227 m^3 kg^{-1},
$\frac{\Delta T}{\Delta h}$ = change of temperature with change in height of the light ray = approximately -0.0065 °K/m standard value,
g = gravitational constant = 9.81 m/s^2.

The 1/r value is then used to calculate refraction-corrected horizon and target angles for Eq. 3, α_c and θ_c, as follows:

$$\alpha_c = \text{atan}\sqrt{2h_m\left(\frac{1}{1000R_E} - \frac{1}{r}\right)}, \tag{10}$$

and

$$\theta_c \approx \theta + \frac{1000D}{2r}, \tag{11}$$

with all terms defined as for Eqs. *7* to *9* above. Under normal survey conditions, the true distance, *D*, to the target in Eq. *11* will be unknown, but it can be initially approximated using Eq. 3, and then iterated to the desired precision.

The values of α_c and θ_c were used in Eq. *3* to produce distances corrected for the effects of refraction using local air temperatures and pressures. An alternative adjustment method used the means of these temperatures and pressures over the entire study area in Eq. *6* to calculate a single *r* value in Eq. *9* representing *average* refraction for the time and region.

Equation *9* uses a temperature gradient of -0.0065 degrees/meter, which is based on standard atmospheric conditions (Leaper and Gordon, 2001; Fleagle and Businger, 1980). The actual gradient along the path the light ray traveled may differ from the standard one, and can be calculated from the observed refraction when true distance to the sighted object is known (Lehn, 1983; Fraser, 1979). Although either positive or negative gradients, indicating increasing or decreasing temperature with height, respectively, are possible near sea level, the typical pattern is decreasing temperature with height (Fleagle and Businger, 1980). Equation *9* produces no change in distances calculated from Eq. *3* at a temperature gradient of approximately -0.034 degrees/meter,

the gradient at which the decreasing temperature with height balances the effect of decreasing pressure to produce a constant density of air (refraction increases as temperature decreases and pressure increases). When air density is constant, no refraction occurs. Refraction will cause underestimates of distance from Eq. *3* as gradient becomes more positive from -0.034, and overestimates of distance for gradients more negative.

We allowed $\Delta T/\Delta h$ in Eq. *9* to be an adjustable variable, and used the criterion of minimum logarithmic mean squared error between distances from reticles and radar (minimum s_2^2 from Eq. *6*) to determine the most likely gradient present during each series of measurements taken with the same air temperature and pressure on one day. Sixteen such series of measurements were made from the *Jordan* and 14 from the *McArthur*. These sets of measurements made under similar environmental conditions to targets over a range of distances produced an estimate of the temperature gradient for each day. This allowed us to estimate the expected effect of refraction on reticle measurements due to the average temperature gradient, as well as air temperature and pressure, in the region.

Empirical Adjustment of α_*

An alternative, simple method of modifying Eq. *3* was to fit an α value for the dip of the horizon, α_*, that produced the minimum root mean squared error for the logarithms of distances from reticles relative to radar (minimum s_2, Eq. *6*). This incorporated any differences, averaged over all target distances, between the theoretical calculations (geometry or refraction) and radar into a single term.

Regression-based Adjustments to Distances from Reticles

Two approaches using least-squares regression to adjust distances from reticles to those from radar were examined. One was numerical and did not use the refraction adjustments. The other was explanatory and attempted to account for variability remaining after refraction had been removed.

Numerical approach. This approach adjusted the distances from reticles calculated using Eq. *3* to radar without attempting to model the physical process underlying the measurements. Correction factors were developed using either distance from radar, or expected vertical angle for the given distance from radar, to predict the observed distance or angle using reticles. Two sets of regression coefficients were thus obtained, producing two different adjustments. In each case, rearrangement of terms provided the correction yielding true distance from reticles. The results were compared in terms of the reduction in s_2 between distances from reticles and radar that was achieved by each method.

The first correction used logarithmic transformations of the distances from both reticles and radar to reduce heteroscedasticity. The distance from reticles was based on the height at which the measurements were taken (Eq. *3*), implicitly assuming this height for the reticle measurements. The second numerical method adjusted the vertical angle before distance was calculated. The angle measured with reticles in this method was

regressed against the expected total angle, solved iteratively from Eq. *3* given D_{LH}. This second set of coefficients was used to produce a correction independent of height.

Both numerical correction methods were based on the simple regression:

$$Y = b_0 + b_1 * X + b_2 * \text{ship}, \tag{12}$$

where

Y = 1) logarithm of distance calculated from reticles (d_{LH}) in the first method; or 2) reticle angle, θ, below the horizon in the second method,

X = 1) logarithm of distance measured with radar (d) in the first method; or 2) expected angle below the horizon from Eq. *3* for the measured distance from radar in the second method, and

ship = dummy variable (*Jordan* = 1, *McArthur* = 0).

Models with and without the dummy variable for ship were compared using AIC_c.

The first method used an antilog back-transformation to produce the correction from the log-log regression coefficients. Rearrangement of terms provided a corrected distance from reticles, D_c, from the logarithm of distance from reticles and Eq. *3* (d_{LH}) as follows:

$$D_{c(k)} = E(X_k) = \exp[\frac{d_{LH(k)} - b_0 - b_2 * \text{ship} - s^2/2}{b_1}], \tag{13}$$

for the k = 1 to m paired measurements, where s^2 was calculated as:

$$s^2 = \frac{\sum_{i=1}^{m}[d_{LH(k)} - (b_0 + b_1 * d_k + b_2 * \text{ship})]^2}{m-1}.$$

The $s^2/2$ term in Eq. *13* is based on the property that if the logarithm of x is normally distributed with mean μ and variance σ^2, the expected value of x is $\exp(\mu + \sigma^2/2)$.

In the second method, the rearranged regression coefficients produced a modified angle, θ_m, as:

$$\theta_m = (\theta - b_0 - b_2 * \text{ship})/b_1. \tag{14}$$

This adjustment was simpler than the distance-based correction in that no antilog bias correction term ($s^2/2$ in Eq. *13*) was required. The modified reticle angle from Eq. 14 was then used in Eq. *3* to calculate corrected distances from reticles. Note that the *b* coefficients in Eqs. *13* and *14* have different values.

Explanatory approach. This approach used regression to produce a model of factors influencing reticle measurements from the two ships after refraction had been accounted for. Ship, Beaufort sea state, swell height, and a relative motion code (upswell, downswell, trough) were recorded during the paired radar and reticle measurements. Distances from reticles calculated using Eq. *3* were adjusted for refraction based on average temperature and pressure and the fitted gradient. Then the ratio of distance from reticles adjusted for refraction to distance from radar was predicted using the additional explanatory variables. Twenty-four linear models using combinations of these variables to predict the reticle/radar distance ratio were ranked based on minimum AIC_c score. The full model including all variables for the ratio, *R*, of refraction-corrected distance from reticles to distance from radar, was:

$$R = b_0 + b_1 v + b_2 f + b_3 fv + b_4 m_1 + b_5 m_2 + b_6 w + b_7 fw + b_8 vw, \qquad (15)$$

where
v = vessel category (1 = *Jordan*, 0 = *McArthur*)
f = Beaufort sea state (continuous)
m_1 = motion category (1 = trough, 0 = downswell, upswell)
m_2 = motion category (1 = upswell, 0 = downswell, trough)
w =swell height (continuous, in feet).

With the ratio of refraction-corrected reticle to radar distance as the dependent variable, the explanatory variables in the regressions represented additional bias beyond the adjustments for refraction. As in the numerical approaches, rearrangement of terms provided an adjusted distance. A final model was selected from among those with the lowest AIC_c scores based on the trade-off between field data requirements and the size of the improvement obtained by using more complicated models to adjust distances from reticles.

Comparisons between adjustment methods

Different subsets of the entire database were adjustable by different methods. Thus a single comparison of all models given the same data by a likelihood method such as AIC was not performed. Instead the adjusted values were compared in terms of: 1) the proportional reduction in s_2 between distance from reticles and radar that was achieved by the method: 2) absolute differences in the distances produced by the different adjustments; and 3) the possible overfitting of a particular dataset by the numerical methods compared to adjustments that were based on a physical model.

RESULTS

Horizontal Angles

The frequency histograms for the 1998-2000 surveys using 25X and non-25X horizontal sighting angles both indicated some rounding to 5-degree increments (Figure 1). In addition, large spikes were found at 5 and 10 degrees in sightings made with 25X

binoculars and at 45 degrees in non-25X sightings. More sightings were made at small angles than at large angles. The mean 25X sighting angle was 35.3 degrees and the mean non-25X angle was 35.8 degrees. These patterns of rounding were generally found in the angle frequencies reported by individual observers as well as for the sightings restricted to only those containing spotted or spinner dolphins, the species targeted by the surveys.

Autocorrelations within the 5-degree lags were greater than for other lags in both the 25X and non-25X measurements, indicating rounding. The autocorrelation coefficients for the 5 degree lags were higher (Figures 2a, 2b) and the Z' tests indicated these differences were significant. For both 25X and non-25X angles, smearing over ±2 degrees ($\Delta\rho = 4$) was sufficient to remove the rounding effects (Tables 4, 5).

The effect of increasing the range of the smearing was to increase the overall autocorrelation between lags as well as smooth over the differences between lags (Figure 2). The predominant feature of the non-25X histogram, the spike at 45 degrees (Figure 1b) continued to be visible as a central hump in the frequency distribution until the data were smeared to ±15 or ±20 degrees. This level of smearing was essentially randomizing the data. Since the objective of removing the repeating spikes was achieved by ±2 degrees of smearing, this was chosen as the optimal level of smearing for the non-25X sightings as well.

The mean standard deviation of the horizontal angle measurements to a common target in the radar target database was 1.5 degrees. This indicates that for unbiased measurements, an interval ± 3 degrees of the measured angle will contain the true angle approximately 95% of the time.

Reticle Angles and Distance Conversion

Reticles were rounded at two different intervals in the field surveys, at every 0.2 reticles for measurements ≤ 2 reticles and every 0.5 reticles when all measurements were considered (Figures 3, 4, Tables 6, 7). The rounding at 0.2 reticles was eliminated by smearing over ± 0.05 reticles ($\Delta\rho = 0.1$). The half-reticle rounding was eliminated by smearing ±1.5 reticles.

In the paired radar and reticle measurements, reticle readings fell rapidly with increasing distance to the target (Figure 5). The reticle values assigned by observers to the radar targets ranged from 0 (the horizon) to 20.5 reticles. Four of the 1606 measurements were assigned reticle values of zero, and two were assigned reticles less than 0.1, normally the minimum value used on the field surveys (observers are instructed to wait until mammals are 0.1 reticles from the horizon or closer, as further distances cannot be adequately discriminated using 25X reticles). These six nonstandard measurements were not used in subsequent analyses.

Twenty-four measurements made from the *McArthur* on one day were anomalous. These formed a cloud of overestimated target distances between 1 and 4 km and were visibly distinct from the general pattern. They were collected heading into the swell

during Beaufort 5 conditions. One hundred and eleven measurements made from the *McArthur* on other days under these conditions did not display this pattern of overestimated distances. There appears to have been a recording error for these data, and along with the six points already mentioned, they were not included in subsequent analyses. This left 1,576 paired measurements of distance using reticles and radar.

Equation *3* provided the best fit of reticles against radar among the formulas tested (Fig. 6). The biases evident in the fits of the Smith 1982 (Fig. 6a) and Buckland 1993 (Fig. 6b) formulas match those discussed from a theoretical perspective in Lerczak and Hobbs (1998). The Bowditch 1995 formula underestimated distances (Fig. 6c).

Although Eq. *3* produced distances from reticle measurements that agreed well with radar, there was a slight tendency to underestimate distances to targets near the horizon (Fig. 6d). For the farthest targets, distance was underestimated by about 10%. This underestimate was not evident in reticle measurements of targets closer than 5 - 6 km.

A difference between ships in recording reticles for targets near the horizon was apparent, with measurements made from the *Jordan* closer to expectations than those from the *McArthur* (Fig. 7). Distances to targets near the horizon were underestimated from both ships, but the underestimate from the *McArthur* was more pronounced. The mean target distance recorded for each of reticles 0.1 to 0.5 was greater on the *McArthur* than on the *Jordan* (Table 8). Yet the observation platform on the *McArthur* was lower, so by geometry the distances for each reticle should be less than for the *Jordan*. A two-tailed *t*-test, allowing unequal variances, of the differences between means for the ratios of Eq. 3 distance to radar for the two ships had a *p*-value of 0.02. The *Jordan* mean distance was 97.6% of radar and the *McArthur* was 95.8%. The frequency distribution of the ratios of Eq. *3* measurements against radar displays the difference between ships that is summarized in the *t*-test (Fig. 8).

The mean standard deviation of the logarithms of replicate measurements of distance from Eq. *3* to a single target in the radar data (s_1 from Eq. *5*, which is precise but biased to the extent the expected mean of distances from reticles do not equal true distances) was 0.0719. This 0.0719 value corresponds to a 95% confidence interval of between 0.87 and 1.15 km for a target at 1 km, and between 6.95 and 9.21 km for a target at 8 km (Eq. *4*). Measurements from the *Jordan* were more precise than those from the *McArthur* (s_1 = 0.0683 versus 0.0767, respectively). These values serve as best-case estimates of the precision possible from reticle measurements under field survey conditions once bias has been removed.

Table 9 lists the variability including bias (s_2 from Eq. *6*) of the various methods of adjusting distances from Eq. *3* compared to radar. The s_2 value of the unadjusted distances from Eq. *3* for the combined dataset was 0.1227 (Method #31 - Table 9). The *Jordan* value was 0.1002 and the *McArthur* value was 0.1482. Different subsets of the data were adjustable using the alternative methods – some adjustments produced undefined values for very small reticle angles, for instance. The ratio of adjusted to

unadjusted distances from reticles using each method is listed in the table along with the unadjusted variability and the number of measurements that produced a numerical result for each adjustment method.

Correcting Distances from Reticles Based on Refraction

Adjusting α only: The refraction-adjustment method of substituting α_B (Eq. *7*) for the above-horizon angle without a corresponding adjustment to the target angle overcorrected the downward bias of Eq. 3 relative to radar. It produced a larger error (s_2) than the unmodified equation for the *Jordan* (Method #23 - Table 9), and was undefined for angles of 0.1 reticle (Figure 10a). Although the α_B values were comparable to the α_c produced using Eq. *10* (see below), the lack of a corresponding increase in target angle, θ_c (Eq. *11*), resulted in Eq. *3* becoming the square root of a negative number when α_B was used with reticle values less than 0.12 from a 10.4 m platform.

Adjusting both α and θ: Adjusting α and θ in Eq. *3* for local refraction effects (α_c and θ_c in Eqs. *10* and *11*, respectively) reduced the near-horizon downward bias (Fig. 9a) and improved the fit of distances from reticles to those from radar. The root mean squared error (s_2) for the combined ships was 0.1160 using the standard temperature gradient (Method #25 - Table 9), 95% of the value for the unadjusted distances. The transformed dip values, α_c, using local air temperatures and pressures ranged between 0.00165 and 0.00169. The target angles, θ_c, were increased relative to θ by approximately 10^{-8} radians. The effects of these small increases in vertical angles on the calculated distance were most evident for targets near the horizon.

Air temperatures and pressures during the measurements ranged between 15.7 and 31.5 ºC and between 1008 and 1019 mb, respectively. Both ranges are typical for the eastern tropical Pacific from July to December (da Silva et al., 1994). These produced 1/r values between 2.38×10^{-8} and 2.67×10^{-8} when combined with the standard temperature gradient of -0.0065 degrees/meter. Figure 9b shows the effect this range of 1/*r* values had on correcting distances from reticles for refraction from a 10.4 m platform. By 8 km, the uncorrected distance from Eq. *3* varied between about 93% and 94% of the corrected value. The approximately 1% difference attributable to local conditions suggested a standard correction based on average conditions would provide most of the improvement obtainable using local temperatures and pressures (see also Leaper and Gordon, 2001).

The adjustments for refraction using locally measured temperatures and pressures had a larger effect on the *McArthur* than on the *Jordan* (Table 9). Refraction effects were insufficient to account for all of the underestimate of target distances on the *McArthur*, however. Extreme air temperatures below 0 ºC, or pressures above 2,000 mb (the normal maximum air pressure at sea level worldwide is 1040 mb, averaging 1013 mb - Fleagle and Businger, 1980) would be required to produce refractive effects sufficient to explain the underestimates of the size recorded from the *McArthur*.

Using the average 1/r value of 2.48×10^{-8}, based on mean temperatures and pressures and the standard temperature gradient from both ships to calculate an average

refraction effect reduced the error from the unadjusted values (Method #10 - Table 9). The value of s_2 from Eq. *6* was 0.1114 for both ships combined. The downward bias of Eq. *3* was reduced (Fig. 10b), although measurements from the *McArthur* continued to underestimate true distance. Iterating Eq. *1*1 three times was sufficient to achieve convergence to a precision of 0.1 km. For example, the estimated distance at 0.1 reticle for a 10.7 m high platform changed from the unadjusted value of 7.98 km, to 8.66 km, to 8.53, and then stabilized at 8.55 km.

Although using either locally-measured or averaged air temperatures and pressures with the standard temperature gradient improved the fit of reticles to radar for both ships combined, this was not true when local temperatures and pressures were combined with the standard gradient for the ships individually. The root mean squared error of the adjusted *McArthur* measurements was improved (90% that of the unadjusted values, Method #27 - Table 9). The *Jordan* ratio (101%, Method #26 - Table 9), however, indicated a slight decrease in accuracy after the refraction adjustment. This may have been due to the use of the standard temperature gradient ($\Delta T/\Delta h$ = -0.0065), discussed below.

Estimating the local value of the $\Delta T/\Delta h$ term in Eq. *9* by allowing it to be an adjustable variable produced daily temperature/height gradients ranging from -0.05 to 0.03 degrees/meter for the *Jordan* (16 series of measurements made on the same day, temperature and pressure, Table 10) and from -0.05 to 0.05 degrees/meter for the *McArthur* (14 series). Although the ranges of measured temperatures and pressures from the two ships were similar, 11 of the *McArthur* series fittings produced positive temperature gradients, while only 2 of the *Jordan* gradients were positive. The average gradient from the *Jordan* was -0.02 degrees/meter, while the *McArthur* average was 0.01.

Because reticle measurements from the *McArthur* appeared to underestimate distances more than expected from refraction alone, fitting the gradient term to measurements made from the *McArthur* likely produced a positive bias in the estimated gradient, overfitting additional error than just the portion due to refraction. The *Jordan* average gradient of -0.02 is probably a better value for the average rate of change in air temperature in the first 10 m above the sea surface in the eastern tropical Pacific in July-December than either the *McArthur* value, or the -0.0065 value based on a standard atmosphere.

Using a temperature gradient of -0.02 degrees/meter with the mean measured temperature (25.2 deg) and pressure (1012.4 mb) in Eqs. *8* and *9* produced a 1/r value of 1.27×10^{-8} instead of 2.47×10^{-8}. This resulted in a smaller adjustment to distances from reticles than the standard gradient of -0.0065. The *Jordan's* value of s_2 using the -0.02 gradient was 0.0980 (Method #29 - Table 9). The improvement achieved by estimating two parameters, gradient and σ^2, from the *Jordan's* data over using the standard gradient (estimating only one parameter, σ^2) was assessed using AIC. With s_2^2 as the maximum likelihood estimator of σ^2 (Burnham and Anderson 1998, pg.48), ΔAIC was 44 using the -0.02 versus the -0.0065 gradient, indicating substantial improvement using the -0.02 degrees/meter gradient for the *Jordan*.

Using the local temperatures, pressures, and fitted temperature gradients for each daily series of measurements (16 sets of measured temperatures and pressures and fitted gradients) to adjust the *Jordan* reticle values produced an s_2 of 0.091, lower than any of the s_2 values achieved using the methods summarized in Table 9. This method of calculating the local temperature gradient would not be feasible under normal survey conditions, however, when the true distances would not be known and so the local gradient could not be calculated for each sighting. Under normal circumstances an average gradient would need to be used.

Empirical Adjustment of α_*

A fitted α_* value of 0.00175, intermediate between Eq. *3* and either the standard Bowditch value of α_B or the α_c adjustments for refraction, produced a minimum s_2 of 0.1152 for the combined ship data (Method #16 - Table 9). The difference between ships was evident in the effect of using this α_* value. Reticle measurements from the *Jordan* tended to be overcorrected while those from the *McArthur* were undercorrected (Figure 11). Fitting separate values for each ship resulted in α_* values of 0.00179 for the *Jordan* and 0.00170 for the *McArthur*. These ship-specific values produced unbiased measures of distance using reticles (Fig. 12) for these data with an s_2 of 0.1099 (Method #4 - Table 9).

The s_2 values after adjusting α_* separately for the two ships were 0.0970 for the *Jordan* versus 0.1255 for the *McArthur* (Method #'s 5 and 6 in Table 9, respectively), reflecting the greater variability for the latter. *McArthur* measurements were made in rougher conditions, with Beaufort sea states from 2 -5 compared to 1 - 4 on the *Jordan*. When measurements from the same Beaufort states (2-4) on the two ships were compared the *McArthur* continued to be more variable (s_2 = 0.1102 versus 0.0959).

Correcting Distances Based on Regression

Numerical corrections. For both regressions, the full model (Eq. *12*) including a ship effect had substantially more support than the submodel without ship (ΔAIC_c = 78.8 for the distance regression and 12.1 for the target angle regression - Table 11).

The first regression, predicting logarithm of distance from reticles from the logarithm of distance from radar (Fig. 13a), reduced the heteroscedasticity evident in Figure 6d (see residuals in Fig. 13b). Rearrangement of terms as described in Eqs. *10-12* produced a corrected distance, D_c, of:

$$D_c = \exp((d_{LH}+0.01176-0.04873*\text{ship}-0.00550)/0.94958), \quad (16)$$

where

d_{LH} = logarithm of uncorrected distance calculated from Eq. *3*.

Rearrangement of regression coefficients for the alternative method of regressing the reticle angle instead of the distance produced the modified angle, θ_m, of:

$$\theta_m = (\theta - 0.00018 + 0.00011*\text{ship})/0.99932. \quad (17)$$

The modified angle in Eq. *17* was then used in Eq. *3* to produce the modified distance from reticles.

The s_2 value using the adjusted distances from Eqs. *13* and *14* were 0.1106 and 0.1119, respectively (Method #'s 7 and 13 - Table 9). The effect of the correction based on Eq. *16* was to remove the downward bias of unmodified Eq. *3* for the farthest distances (Figure 14). The θ_m angle method of Eq. *17* also improved the fit over uncorrected reticles, but not as well as Eq. *16*.

Explanatory regression models: The 24 models representing subsets of Eq. *15* were applied to the distances from reticles and Eq. *3*, adjusted for refraction using average air temperatures and pressures and the fitted gradient. Motion codes were only recorded for 1070 of the measurements, so only these records could be compared among models using AIC_c scores. ΔAIC_c scores among the regression models ranged from 0 to 98.6 (Table 12). AIC_c and AIC (the large-sample version of this score) values were nearly identical. Using either estimate of the distance between model and data produced similar results.

The top seven models had from 4 to 9 coefficients (Table 13), and all included effects for ship, Beaufort, and an interaction between ship and Beaufort. The simplest of these, the 4-parameter model, was 6.2 ΔAIC_c above the model with the lowest score. The difference between the model with the lowest score and the second ranked model was 1.0 ΔAIC_c. Models with differences in AIC_c scores (ΔAIC_c) within about 2 ΔAIC_c of one another have roughly comparable support (Burnham and Anderson 1998), so by this criterion, Models 1 and 2 were the best supported by the data of those considered. Differences in the distances from reticles produced by the seven top models were examined to determine the practical effect of adding variables to the simplest model on improving accuracy.

Differences in the accuracy of distances from reticles produced among the top seven regression models were negligible, once any one of them was selected (Table 14). The difference between the measurements corrected only for refraction and those additionally adjusted by any of the regression models was larger than differences among models. The maximum difference between unadjusted distances from Eq. *3* and those adjusted for refraction was 0.28 km, with an average difference of 0.10 km. The maximum difference between Model 7 and refraction-adjusted distances was 0.56 km, averaging 0.12 km. But the maximum difference between the 6-parameter Model 1 and the 4-parameter Model 7 was only 0.25 km, averaging 0.03 km. Given the inherent variability in reticle measurements (Table 15), the point of diminishing returns appears to have been reached with Model 7.

Model 7 was selected as the most practical of the seven models because of its relatively simple data needs. The adjusted distance, D, from the refraction-corrected distance from reticles, D_{refract}, using Model 7 was:

$$D = D_{refract} / (1.0138 - 0.0156*f - 0.0531*v + 0.0281*f*v), \quad (18)$$

with f and v defined as in Eq. *15* as Beaufort sea state and vessel, respectively.

This model, applied to the refraction-corrected reticle measurements, improved the fit of reticles to radar (Figs. 15, 16, Method #1 - Table 9). The mean ratios of distance from reticles to radar for targets ± 0.5 km around each of distances 1 to 8 km approached 1 as distances from reticles were adjusted, first for refraction, and then using Model 7 (Table 15). These ratios provide values around which to center the confidence intervals for the given target distance in order to report both precision and accuracy for targets at those distances (Table 16).

Table 16 summarizes the improvements in precision and accuracy in radial distances achieved with the adjustments for refraction both with and without the additional, ship-specific corrections. The left, "unadjusted" columns indicate the 95% confidence interval for a target at the given distance based on Eq. *3*. This interval includes all the sources of bias and variability that were present during the tests. When the measurement process was unadjusted for any of these sources of error, the 95% confidence interval for an object at 8 km ranged from 5.6 to 9.0 km (mean = 7.1 km, from 8 km * 0.89 [Eq. *3* / radar ratio from Table 15]), using a continuous representation of the reticle scale. "Measurement error," at the right side of Table 16 is based on the 0.0719 value of s_1 from replicate measurements to a single target under the same set of conditions at a single place and time. This best-case value indicates that if all sources of non-random error were removed, a target at 8 km would be measured within the interval 6.9 to 9.2 km (mean = 8.0 km) 95% of the time. The intermediate columns in Table 16 show the improvements in accuracy achieved in measurements of radial distance using the adjustments discussed in this study. The 95% confidence intervals improve both in terms of precision and reduced bias (Fig. 16).

DISCUSSION

The objective of this study was to identify and adjust for systematic measurement errors of the angles and distances to sightings in SWFSC shipboard surveys that can produce bias in line-transect estimates of abundance. One step in this process was to recognize the amount of change required to have a practical effect on measurements of perpendicular distances, as opposed to effects that may be statistically significant but do not produce a meaningful correction to the measurements.

Rounding of Horizontal Angles and Reticles

The effect of the amount of rounding of horizontal angles and reticles found in the 1998-2000 survey data on the final estimates of mammal density and abundance is

difficult to predict. The extent of rounding was much less than in the minke whale data for which Butterworth (1982) developed the smearing technique. In particular, rounding to perpendicular distance zero, which is known to be problematic (Buckland et al., 2001), was not apparent in the survey data. The rounding of horizontal angles was less than the precision obtainable by duplicate measurements, an indication that rounding might not produce an observable effect on the calculated frequencies, and that smearing was therefore not necessary.

The actual estimates for 1998-2000 will be made for small subsets of the entire database examined here, for instance, eastern spinner dolphins in one sampling area for one year. Estimates based on these subsets may be more susceptible to small artifacts of data collection than apparent from the combined sightings over the entire the 3-year period. Comparison of the estimates produced from the original data and from smeared data provide a measure of the importance rounding has on the final estimates for a particular dataset.

Radial Distances

Modification of Eq. *3* is required if unbiased distances are to be obtained at all reticle values used during the surveys. The underestimate of near-horizon distances by the original equation would have a small but consistent positive bias on estimated density and abundance. About 6-7% of the sightings from the 1998-2000 surveys were recorded at each of 0.1, 0.2 and 0.3 reticles, distances for which the underestimate would be noticeable. Unadjusted reticle measurements would underestimate radial distance for about 20% of the 1998-2000 sightings by from 2 to 10%.

Roughly half of the underestimate was correctable by incorporating the effects of refraction on reticle measurements into the distance calculations. Use of an average refraction term provided most of the bias reduction potentially obtainable by measuring air temperatures and pressures individually for each sighting. Refraction was insufficient to explain all of the underestimate of distances produced from reticles, however. Distances from reticles to near-horizon targets were less than expected from both ships based on ship height, refraction, and distance from radar, particularly on the *McArthur*. Refraction-corrected *Jordan* distances were closer to expectations. The underestimate on the *McArthur* comprised the bulk of the remaining difference between distances from reticles and radar for both ships combined, once refraction had been accounted for. The apparent difference between ships complicates the adjustment required to remove this final portion of bias.

The method of empirically fitting the α_* value for each ship separately to radar is one option for providing a ship-specific adjustment. For the *McArthur*, this produced the second greatest reduction in mean squared error of any adjustment method (Method #6 - Table 9). Using the same fitting technique with the *Jordan* performed less well. As with all the numerical methods, it doesn't make use of the known effects of refraction, and there is a danger of overfitting artifacts in the data with constants that have no physical

interpretation. The regression models incorporating explanatory variables were selected over the numerical methods as the best adjustment approach.

In addition to ship, Beaufort sea state, and their interaction, AIC_c indicated swell height, and a pairwise interaction between ship and swell, were significant variables. A limit to the usefulness of the adjustments to reticle measurements was reached, however, beyond which additional factors that were statistically significant provided little practical benefit.

The *McArthur* was the more active of the two ships under similar sea conditions. The adjustment model indicated that distance from reticles increased with Beaufort on the *McArthur*, but not on the *Jordan*. If differences in ship responsiveness resulted in observers reading reticles differently as Beaufort sea state increased, for instance tending to read more at the top of a swell on the *McArthur* than on the *Jordan*, the effective height on the *McArthur* would increase and the results observed in the data would be obtained. Gordon (2001) discusses the opposite effect of ship rolling or heeling, which will result in distances being overestimated. This heeling effect was not apparent in our data, however.

A final complicating issue that bears on extending the results of this study into the future is that stabilizers were added to the *McArthur* in 2001, greatly reducing its roll compared to the period when the data reported here were collected. Thus, adjustments for ship-specific differences in responsiveness may no longer apply. The adjustment for refraction, however, warrants consideration anytime distance measurements are to be made near the horizon with any angle-based device.

ACKNOWLEGEMENTS

We thank the officers and crew of the NOAA Ships *McArthur* and *David Starr Jordan* for their professional support during this research, for providing the radar distances to the targets, and conducting small boat operations. We also thank the observers who made the reticle measurements. Drs Bob Mohn, Paul Medley, and Karin Forney reviewed earlier versions of the manuscript. This analysis was made possible through funding by the International Dolphin Conservation Program Act to the Southwest Fisheries Science Center.

LITERATURE CITED

Barlow, J. and T. Lee. 1994. The estimation of perpendicular sighting distance on SWFSC research vessel surveys for cetaceans: 1974 to 1991. U.S. Department of Commerce, NOAA Technical Memorandum. NMFS-SWFSC-207. 46 pp.

Bowditch, N. 1995. The American Practical Navigator. U.S. Defense Mapping Agency Hydrographic/Topographic Agency. Bethesda, Maryland.

Buckland, S.T., D.R. Anderson, K.P. Burnham, and J.L. Laake. 1993. Distance Sampling: Estimating Abundance of Biological Populations. Chapman and Hall, London. 446 pp.

Buckland, S.T., D.R. Anderson, K.P. Burnham, J.L. Laake and L. Thomas. 2001. Introduction to Distance Sampling: Estimating Abundance of Biological Populations. Oxford University Press.

Burnham, K.P. and D. R. Anderson. 1998. Model Selection and Inference: A Practical Information-Theoretic Approach. Springer-Verlag. 353 pp.

Butterworth, D. S. 1982. On the functional form used for g(y) for minke whale sightings, and bias in its estimation due to measurement inaccuracies. Rep. Int. Whal. Commn. 32: 883-888.

da Silva, A. M., C. G. Young and S. Levitus. 1994. Atlas of Surface Marine Data 1994 Volume 2: Anomalies of Directly Observed Quantities. NOAA Atlas NESDIS 7.

Fleagle, R. G. and J. A. Businger. 1980. An Introduction to Atmospheric Physics. 2nd ed. Academic Press, New York. xiv+432 pp.

Fraser, A. B. 1979. Simple solution for obtaining a temperature profile from the inferior mirage. Applied Optics. 18:1724-1731.

Gordon, J. C. D. 1990. A simple technique for measuring the length of whales from boats at sea. Rep. Int. Whal. Commn. 40:581-588.

Gordon, J. 2001. Measuring the range to animals at sea from boats using photographic and video images. Journal of Applied Ecology 38:879-887.

Hammond, P. S. 1984. An investigation into the effects of different techniques of smearing the IWC/IDCR minke whale sightings data and of the use of different models to estimate density of schools. Rep. Int. Whal. Commn. 34: 301-307.

Jaramillo-Legorreta, A. M., L. Rojas-Bracho, and T. Gerrodette. 1999. A new abundance estimate for vaquitas: First step for recovery. Mar. Mamm. Sci. 15(4):957-973.

Kinzey, D., T. Gerrodette, J. Barlow, A. Dizon, W. Perryman, P. Olson and A. Von Saunder. 1999. Marine mammal data collected during a survey in the eastern tropical Pacific Ocean aboard the NOAA ships *McArthur* and *David Starr Jordan* and the UNOLS ship *Endeavor* July 31 – December 9, 1998. NOAA-TM-NMFS-SWFSC-283. 113 pp.

Kinzey, D., T. Gerrodette, J. Barlow, A. Dizon, W. Perryman and P. Olson. 2000. Marine mammal data collected during a survey in the eastern tropical Pacific Ocean aboard the

NOAA ships *McArthur* and *David Starr Jordan* July 28 – December 9, 1999. NOAA-TM-NMFS-SWFSC-293. 89 pp.

Kinzey, D., T. Gerrodette, A. Dizon, W. Perryman, S. Rankin and P. Olson. 2001. Marine mammal data collected during a survey in the eastern tropical Pacific Ocean aboard the NOAA ships *McArthur* and *David Starr Jordan* July 28 – December 9, 2000. NOAA-TM-NMFS-SWFSC-303. 100 pp.

Kinzey, D. and T. Gerrodette. 2001. Conversion factors for binocular reticles. Mar. Mamm. Sci. 17(2):353-361.

Leaper, R. and J. Gordon. 2001. Application of photogrammetric methods for locating and tracking cetacean movements at sea. J. Cet. Res. Man. 3(2):131-141.

Lehn, W. H. 1983. Inversion of superior mirage data to compute temperature profiles. J. Opt. Soc. Am. 73:1622-1625.

Lerczak, J. A. and R. C. Hobbs. 1998. Calculating sighting distances from angular readings during shipboard, aerial, and shore-based marine mammal surveys. Mar. Mamm. Sci. 14(3):590-599.

Smith, T. 1982. Testing methods of estimating range and bearing to cetaceans aboard the R/V *D. S. Jordan*. U.S. Department of Commerce, NOAA Technical Memorandum NOAA-TM-NMFS-20. 30 pp.

Thomas, L., J.L. Laake, J.F. Derry, S.T. Buckland, D. L. Borchers, D.R. Anderson, K.P. Burnham, S. Strindberg, S. L. Hedley, M.L. Burt, F.F.C. Marques, J. H. Pollard, and R.M. Fewster. 1998. Distance 3.5. Research Unit for Wildlife Population Assessment, University of St. Andrews, UK. Available: http://www.ruwpa.st-and.ac.uk/distance/

Zar, J. H. 1984. Biostatistical Analysis. Prentice Hall. 662 pp.

Table 1. Summary of field survey measurements. Types of horizontal angle and distance measurements recorded on-effort during SWFSC line-transect surveys from 1998 to 2000. Measurements were obtained from a total of 4,307 sightings.

Data type	No. of Measurements
25X horizontal angles	3,941
25X vertical angles (reticles)	3,986
25X reticles ≤ 2 reticles	2,791
non-25X horizontal angles	365
non-25X distances from reticles	321

Table 2. Summary of radar target measurements indicating the numbers of replicated horizontal angles and reticles measured to a single target by different observers. A total of 1606 measurements were made of 551 individual targets. No horizontal angle measurements were recorded for 34 of the targets.

Replicates/target	Horizontal angles	Reticles
1	5	4
2	45	45
3	464	499
4	1	1
5	1	1
6	1	1

Table 3. Angle-distance formulas: D = distance in km, h = observer eye height in meters above sea level, θ = angle from horizon to target in radians, α = angle above horizon to horizontal tangent in radians. The Bowditch (1995) equation was modified from its original form expressing angle in terms of distance by rearranging terms. Observer height, (h_f), is in feet, k_1 = 6076.1 and k_2 = 8268.

Reference	Formula
Lerczak and Hobbs (1998)	$D = (6371+h/1000)\sin(\theta+\alpha)$ - sqrt[6371^2 - $((6371 + h/1000)(\cos(\theta+\alpha))^2)$]
Smith (1982)	$D = 1.852*(h/1852)\tan(\text{atan}(89.173/\text{sqrt}(h/1852))-\theta)$
Buckland *et al.* (1993)	$D = (0.001h)/\tan(\text{acos}(6371/(6371+(0.001h)))+\theta)$
Bowditch (1995)	$D =1.852\{\tan(\theta+\alpha)k_1k_2$ - sqrt[$(-\tan(\theta+\alpha)k_1k_2)^2-4h_fk_1k_2$]}$/(2k_1)$

Table 4. 25X horizontal angle rounding and smearing of field survey data. Five-degree rounding test (Eq. *1*). Autocorrelation coefficients and Z' scores of original angles and of angles smeared (Eq. *2*) over $\Delta\rho = 2$, 3, and 4 degrees (additional smearing at $\Delta\rho > 4$ not shown). Statistics for smeared data are averages of 20 runs. Z' scores less than -1.645, indicated by asterisks, represent 95% probability that 5 degree lags have higher autocorrelation than the tested lag (the original rounding spikes remain detectable).

	original angles			**$\Delta\rho = 2$**			**$\Delta\rho = 3$**			**$\Delta\rho = 4$**	
Lag	**r**	**Z'**		**r**	**Z'**		**r**	**Z'**		**r**	**Z'**
1	0.346	-4.500	*	0.817	0.782		0.769	-0.224		0.848	1.096
2	0.544	-2.865	*	0.743	-0.460		0.782	-0.007		0.837	0.850
3	0.503	-3.222	*	0.729	-0.662		0.754	-0.467		0.825	0.586
4	0.320	-4.646	*	0.766	-0.124		0.748	-0.548		0.806	0.226
5	0.782	0.000		0.773	0.000		0.783	0.000		0.794	0.000
6	0.303	-4.745	*	0.717	-0.826		0.699	-1.205		0.752	-0.664
7	0.385	-4.132	*	0.640	-1.736	*	0.641	-1.873	*	0.742	-0.824
8	0.461	-3.525	*	0.624	-1.904	*	0.673	-1.523		0.727	-1.024
9	0.173	-5.578	*	0.670	-1.403		0.617	-2.123	*	0.692	-1.461

Table 5. Non-25X rounding and smearing of horizontal angles in the field survey data. Autocorrelation coefficients and Z' scores for 5-degree rounding of original angles, and of angles smeared over 2, 3, and 4 degrees. Statistics for smeared data are averages of 20 runs. Z' scores indicated by asterisks represent 95% probability that 5 degree lags have higher autocorrelation than the tested lag.

	original angles			**$\Delta\rho = 2$**			**$\Delta\rho = 3$**			**$\Delta\rho = 4$**	
Lag	**r**	**Z'**		**r**	**Z'**		**r**	**Z'**		**r**	**Z'**
1	-0.134	-4.305	*	0.459	1.680		0.381	1.128		0.510	3.240
2	-0.098	-4.058	*	-0.059	-1.940	*	0.050	-1.172		0.310	1.656
3	-0.098	-4.044	*	-0.116	-2.311	*	-0.063	-1.904	*	0.166	0.651
4	-0.132	-4.253	*	0.113	-0.816		0.087	-0.926		0.086	0.125
5	0.482	0.000		0.235	0.000		0.226	0.000		0.067	0.000
6	-0.138	-4.273	*	0.053	-1.195		0.030	-1.286		0.023	-0.286
7	-0.099	-4.000	*	-0.168	-2.619	*	-0.134	-2.341	*	-0.013	-0.518
8	-0.099	-1.478		-0.129	-2.355	*	-0.105	-2.144	*	-0.012	-0.510
9	-0.126	-4.152	*	0.076	-1.036		0.046	-1.174		0.009	-0.370

Table 6. 25X reticle rounding and smearing in the field survey data for measurements ≤ 2 reticles. Z' scores are for rounding at 0.2 reticles. Smeared values are averages of 20 runs. Z' asterisks indicate 95% probability that the tested lag had lower autocorrelation than the 0.2 reticles of rounding.

	original reticles			**$\Delta\rho$ = 0.1**	
Lag	**r**	**Z'**		**r**	**Z'**
0.1	0.323	-1.556		0.812	1.620
0.2	0.669	0.000		0.565	0.000
0.3	0.202	-1.935	*	0.460	-0.457
0.4	0.429	-1.107		0.368	-0.802
0.5	0.239	-1.763	*	0.485	-0.343
0.6	0.503	-0.968		0.617	0.301
0.7	0.298	-1.512		0.566	0.005
0.8	0.300	-1.787	*	0.388	-0.825
0.9	0.217	-1.707	*	0.320	-0.895

Table 7. 25X reticle rounding and smearing in the field survey data for measurements at all reticle values. Autocorrelation coefficients for 25X reticles at all reticle values, with Z’ scores computed against 0.5 reticle lags.

	original reticles			**$\Delta\rho$ = 0.1**		**$\Delta\rho$ = 0.2**		**$\Delta\rho$ = 0.3**	
Lag	**r**	**Z'**		**r**	**Z'**	**r**	**Z'**	**r**	**Z'**
1	0.553	-1.805	*	0.884	2.315	0.887	2.363	0.920	3.521
2	0.722	1.046		0.755	-1.717 *	0.761	-1.700 *	0.853	0.324
3	0.505	-2.456	*	0.718	-2.497 *	0.720	-2.576 *	0.798	-1.361
4	0.589	-1.265		0.728	-2.297 *	0.735	-2.277 *	0.811	-0.994
5	0.667	0.000		0.820	0.000	0.824	0.000	0.843	0.000
6	0.579	-1.416		0.802	-0.518	0.804	-0.578	0.861	0.653
7	0.518	-2.271	*	0.745	-1.932 *	0.743	-2.084 *	0.832	-0.384
8	0.490	-2.639	*	0.679	-3.247 *	0.678	-3.380 *	0.807	-1.131
9	0.438	-3.276	*	0.718	-2.496 *	0.723	-2.503 *	0.801	-1.283

Table 8. Mean distances from radar to targets assigned to the given reticle values on the two ships, the distances from Eq. *3* for the angles these reticles represent given the ship's height, and numbers of measurements recorded.

Reticle	**Mean Target Distance Assigned this Reticle from the *Jordan* (ht = 10.7 m)**	**Eq. 3 *Jordan* Distance**	**N_{JORDAN}**	**Mean Target Distance Assigned this Reticle from the *McArthur* (ht. = 10.4 m)**	**Eq. 3 *McArthur* Distance**	**$N_{McARTHUR}$**
0.1	8.0	8.0	42	8.9	7.8	39
0.2	7.1	6.8	72	7.6	6.7	56
0.3	6.4	6.1	68	6.9	6.0	66
0.4	5.7	5.5	88	5.9	5.4	45
0.5	5.4	5.1	63	5.5	5.0	32
0.6	4.9	4.7	53	4.9	4.6	41
0.7	4.7	4.4	41	4.4	4.3	22
0.8	4.3	4.1	57	4.2	4.1	54
0.9	4.1	3.9	26	3.9	3.8	18
1.0	3.9	3.7	45	3.6	3.6	26
1.1	3.6	3.5	18	3.7	3.5	12
1.2	3.4	3.4	38	3.7	3.3	27
1.3	3.2	3.2	9	3.0	3.1	15

Table 9. Improvements in accuracy achieved using the various adjustments to Eq. *3*. Results of 11 adjustment methods are each reported in 3 ways: once representing the two ships combined, and once for each ship individually, for a total of 33 sets ("Method #") of statistics. Table columns indicate: Terms estimated from the data; Equations used in addition to Eq. 3; m = number of the measurements that were adjustable using the adjustment method; Eq. *3* s_2 = root mean squared error between logarithms of distances measured by reticles and radar (Eq. *6*) for the measurements that were adjustable using the adjustment method; Adjusted s_2 = root mean squared error after adjustment; and the ratio of adjusted s_2 to s_2 from unmodified Eq. *3*. Results for each method are sorted by decreasing ratio of adjusted to unadjusted s_2 for the combined data, indicated in bold numbering (smaller ratios are better).

Method #	**Adjustment and Ship(s):**	**Terms**	**Eqs.**	m [1]	**Eq. 3** s_2	**Adjusted** s_2	**ratio** [2]
1	Model 7 + Refraction: average temperature and pressure, fitted gradient, both ships	α_c, θ_c	8-11, 18	1576	0.1227	0.1075	**0.88**
2	Model 7 + Refraction: average temperature and pressure, fitted gradient, *Jordan*	α_c, θ_c	8-11, 18	914	0.1002	0.0950	0.95
3	Model 7 + Refraction: average temperature and pressure, fitted gradient, *McArthur*	α_c, θ_c	8-11, 18	662	0.1482	0.1228	0.83
4	Empirical fit: ship-specific above-horizon angle = 0.00170 or 0.00179, both ships	α_*		662	0.1227	0.1099	**0.90**
5	Empirical fit: ship-specific above-horizon angle = 0.00179, *Jordan*	α_*		662	0.1002	0.0970	0.97
6	Empirical fit: ship-specific above-horizon angle = 0.00170, *McArthur*	α_*		662	0.1482	0.1255	0.85
7	Regression: log-log distance coefficients, both ships	D_c, **b**	13, 16	1576	0.1227	0.1106	**0.90**
8	Regression: log-log distance coefficients, *Jordan*	D_c, **b**	13, 16	914	0.1002	0.0997	0.99
9	Regression: log-log distance coefficients, *McArthur*	D_c, **b**	13, 16	662	0.1482	0.1241	0.84
10	Refraction: average air temperature and pressure, standard gradient, both ships	α_c, θ_c	8-11	1576	0.1227	0.1114	**0.91**
11	Refraction: average air temperature and pressure, standard gradient, *Jordan*	α_c, θ_c	8-11	914	0.1002	0.0973	0.97
12	Refraction: average air temperature and pressure, standard gradient, *McArthur*	α_c, θ_c	8-11	662	0.1481	0.1284	0.87
13	Regression: target angle adjustment, both ships	θ_m, **b**	14, 17	1537	0.1219	0.1119	**0.92**
14	Regression: target angle adjustment, *Jordan*	θ_m, **b**	14, 17	914	0.1002	0.0993	0.99
15	Regression: target angle adjustment, *McArthur*	θ_m, **b**	14, 17	623	0.1481	0.1283	0.87
16	Empirical fit: above-horizon angle = 0.00175, both ships	α_*		1576	0.1227	0.1152	**0.94**
17	Empirical fit: above-horizon angle = 0.00175, *Jordan*	α_*		914	0.1002	0.1018	1.02

[1] The total number of paired measurements was 1576, of which 914 were made from the *Jordan* and 662 were from the *McArthur*. 81 measurements on both ships at 0.1 reticles were undefined when corrected using α_B in Eq. 3. 39 measurements at 0.1 reticles were undefined for the *McArthur* ship height using the θ_m correction.

[2] The ratio of adjusted s_2 to s_2 from unmodified Eq. 3 indicates the improvement achieved using the adjustment method compared to unadjusted values for the same data.

Table 9. Accuracy in distances using adjustment methods (continued)

Method #	Adjustment and Ship(s):	Terms	Eqs.	m [1]	Eq. 3 s_2	Adjusted s_2	ratio [1]
18	Empirical fit: above-horizon angle = 0.00175, *McArthur*	α_*		662	0.1482	0.1316	0.89
19	Refraction: average air temperature and pressure, fitted gradient, both ships	α_c, θ_c	8-11	1576	0.1227	0.1150	**0.94**
20	Refraction: average air temperature and pressure, fitted gradient, *Jordan*	α_c, θ_c	8-11	914	0.1002	0.0961	0.96
21	Refraction: average air temperature and pressure, fitted gradient, *McArthur*	α_c, θ_c	8-11	662	0.1482	0.1369	0.92
22	Refraction: substituting Bowditch above-horizon angle into Eq. 3, both ships	α_B	7	1495	0.1265	0.1200	**0.95**
23	Refraction: substituting Bowditch above-horizon angle into Eq. 3, *Jordan*	α_B	7	872	0.1003	0.1146	1.14
24	Refraction: substituting Bowditch above-horizon angle into Eq. 3, *McArthur*	α_B	7	623	0.1481	0.1253	0.85
25	Refraction: local air temperature and pressure, standard gradient, both ships	α_c, θ_c	8-11	1576	0.1227	0.1160	**0.95**
26	Refraction: local air temperature and pressure, standard gradient, *Jordan*	α_c, θ_c	8-11	914	0.1002	0.1015	1.01
27	Refraction: local air temperature and pressure, standard gradient, *McArthur*	α_c, θ_c	8-11	662	0.1482	0.1335	0.90
28	Refraction: local air temperature and pressure, fitted gradient, both ships	α_c, θ_c	8-11	1576	0.1227	0.1174	**0.96**
29	Refraction: local air temperature and pressure, fitted gradient, *Jordan*	α_c, θ_c	8-11	914	0.1002	0.0980	0.98
30	Refraction: local air temperature and pressure, fitted gradient, *McArthur*	α_c, θ_c	8-11	662	0.1482	0.1399	0.94
31	Unadjusted Eq. 3, both ships			1576	0.1227		**1.00**
32	Unadjusted Eq. 3, *Jordan*			914	0.1002		1.00
33	Unadjusted Eq. 3, *McArthur*			662	0.1482		1.00

Table 10. Temperature gradients estimated from fitting $\Delta T/\Delta h$ in Eq. *7* to minimize the differences in distances from reticles and radar (s_2). Each series of N measurements was taken at the given water temperature, air temperature, air pressure, and ship. Sorted by $\Delta T/\Delta h$ for each ship.

Water temp	**Air temp**	**Air press**	**N**	**$\Delta T/\Delta h$**
David Starr Jordan				
24.6	21.5	1012.9	55	-0.049
20.6	20	1011.3	54	-0.047
30	31.5	1010.8	53	-0.046
18.1	19	1017.4	46	-0.04
20.5	20.2	1017.2	61	-0.039
30.5	30	1008.7	39	-0.036
19.2	19.5	1014	13	-0.031
29.5	29.2	1012	56	-0.031
29.2	27.5	1008	63	-0.023
19.1	21.5	1013.8	63	-0.021
30.2	29.8	1008	54	-0.013
30.1	30	1011	60	-0.009
26.7	24.5	1011.8	70	-0.008
30.1	29.8	1012	114	0.008
29.9	28.1	1011.8	23	0.01
18.3	20.8	1017.5	90	0.029
McArthur				
23.6	26.2	1013.8	42	-0.051
31.4	31.1	1011.1	53	-0.014
26.3	21	1015	47	-0.004
26.5	27	1012.6	83	0.001
23.6	25	1012.9	30	0.002
24.8	24.2	1013.1	39	0.006
24.4	26.1	1011.6	102	0.009
31	30.9	1010.5	53	0.011
24.3	24	1012.8	23	0.012
12.5	15.7	1019.1	54	0.013
28.3	30.2	1009.7	48	0.024
23.6	26.5	1013.2	16	0.034
28.3	29	1008.4	60	0.045
27.9	26.9	1009.9	12	0.052

Table 11. Regression equations and coefficients used in numerical methods for correcting distances from reticles. d_{LH} = logarithm of reticle-based distance from Eq. *3*; d = logarithm of distance from radar; θ = empirical reticle angle; θ_T = theoretical angle below horizon for given target distance, solved numerically from Eq. 3. ΔAIC_c is calculated for the model with and without ship.

Regression equation:	$\boldsymbol{b_0}$	$\boldsymbol{b_1}$	$\boldsymbol{b_2}$	$\boldsymbol{\Delta AIC_c}$
$d_{\mathrm{LH}} = b_0 + b_1 * d + b_2 *$ ship	-0.01176	0.94958	0.04873	78.8
$\theta = b_0 + b_1 * \theta_T + b_2 *$ ship	0.00018	0.99932	-0.00011	12.1

Table 12. ΔAIC_c scores for 24 regression models. The ratio of refraction-corrected distance from reticles (average temperature and pressure, temperature gradient = -0.02) to distance from radar was the dependent variable. The independent variables were: v = vessel category (1=DSJ); f = Beaufort; w = swell height; m1 = motion category (1 = trough); m2 = motion category (1 = upswell). The root squared sum of residuals (SRE = $\sqrt{\text{SSR}/\text{df}}$), and the AIC_c values were calculated based on the 1070 records that included the independent variables required by all models.

Model ID	ΔAIC_c	SRE	df	Model
1	0.0	0.1038	1064	b_0+b_1*w+b_2*f+b_3*v+b_4*f*v+b_5*w*v
2	1.0	0.1037	1061	b_0+b_1*w+b_2*f+b_3*v+b_4*m1+b_5*m2+b_6*f*v+b_7*w*f+b_8*v*w
3	2.1	0.1039	1064	b_0+b_1*w+b_2*f+b_3*v+b_4*f*v+b_5*w*f
4	3.1	0.1039	1063	b_0+b_1*w+b_2*f+b_3*v+b_4*f*v+b_5*w*f+ b_6*v*w
5	5.1	0.1040	1063	$b_0 + b_1$ * v + b_2 * f + b_3 * f * v + b_4 * m1 + b_5 * m2 + b_6 * w
6	5.2	0.1041	1065	b_0+b_1*w+b_2*f+b_3*v+b_4*f*v
7	6.2	0.1042	1066	$b_0 + b_1$ * f + b_2 * v + b_3 * f * v
8	8.2	0.1042	1064	$b_0 + b_1$ * v + b_2 * f + b_3 * f * v + b_4 * m1 + b_5 * m2
9	17.5	0.1048	1067	$b_0 + (b_1 + b_2$ * v) * f
10	28.7	0.1053	1066	b_0+b_1*w+b_2*f+b_3*v
11	29.7	0.1054	1067	$b_0 + b_1$ * f + b_2 * v
12	32.7	0.1055	1066	$b_0 + (b_1 + b_2$ * v) * w + b_3 * f * w
13	33.7	0.1056	1067	$b_0 + (b_1 + b_2$ * v) * w
14	33.7	0.1055	1065	$b_0 + b_1$ * f + b_2 * v + b_3 * m1 + b_4 * m2
15	35.8	0.1057	1067	$b_0 + b_1$ * w + b_2 * v
16	35.8	0.1056	1065	$b_0 + (b_1 + b_2$ * v) * w + b_3 * m1 + b_4 * m2
17	36.8	0.1058	1068	$b_0 + b_1$ * v
18	38.8	0.1058	1066	$b_0 + b_1$ * v + b_2 * m1 + b_3 * m2
19	39.8	0.1058	1065	$b_0 + b_1$ * v + b_2 * w + b_3 * m1 + b_4 * m2
20	89.8	0.1083	1065	$b_0 + b_1$ * w + b_2 * f + b_3 * m1 + b_4 * m2
21	90.7	0.1085	1068	$b_0 + b_1$ * f
22	92.7	0.1085	1066	$b_0 + b_1$ * f + b_2 * m1 + b_3 * m2
23	96.6	0.1088	1068	$b_0 + b_1$ * w
24	98.6	0.1088	1066	$b_0 + b_1$ * w + b_2 * m1 + b_3 * m2

Table 13. Regression coefficients for the 7 top AIC_c - ranked models from Table 12. Regression coefficients for Models 2 and 5 were based on the 1070 records that included motion codes. Coefficients for Models 1, 3, 4, 6, and 7 were based on the full database of 1576 records.

Model ID	b_0	b_1	b_2	b_3	b_4	b_5	b_6	b_7	b_8
1	1.0201	-0.0020	-0.0149	-0.0914	0.0281	0.0122			
2	1.2047	-0.0102	-0.0473	-0.2933	0.0111	-0.0115	0.0662	0.0005	0.0207
3	0.9618	0.0137	-0.0075	-0.0410	0.0265	-0.0023			
4	1.1051	-0.0235	-0.0328	-0.1502	0.0345	0.0045	0.0232		
5	1.1161	-0.1895	-0.0429	0.0614	0.0152	0.0037	0.0048		
6	0.9921	0.0070	-0.0181	-0.0534	0.0311				
7	1.0138	-0.0156	-0.0531	0.0281					

Table 14. Maximum and mean absolute differences in distances (km) produced by the top seven explanatory regression models, the refraction-adjusted (using average temperature and pressure and the fitted gradient) measurements, and distances from unadjusted Eq. 3. Models correspond to Models 1 to 7 in Tables 12 and 13.

Models Compared	**Max. (absolute) difference**	**Avg. (absolute) difference**
Refraction adjusted - unadjusted eq. 3	0.28	0.10
Model_7 - refraction adjusted eq. 3	0.56	0.12
Model_7 - Model_6	0.17	0.03
Model_6 - Model_5	0.19	0.04
Model_5 - Model_4	0.25	0.06
Model_4 - Model_3	0.15	0.02
Model_3 - Model_2	0.20	0.05
Model_2 - Model_1	0.23	0.04
Model_7 - Model_1	0.25	0.03
Model_1 - refraction adjusted eq. 3	0.58	0.13

Table 15. Mean ratios of calculated distance (unadjusted and adjusted by two methods) to distance from radar for targets ± 0.5 km around the given midpoint distance. N = number of targets measured in the interval around the given midpoint. The refraction adjustment used average air temperatures and pressures and the fitted temperature gradient. The final adjustment applied Model 7 to these distances. Bias, the expected overestimate or underestimate in meters for distances calculated to a target at the given distance, is reported for each method.

		Equation 3		**Refraction-adjusted**		**Final-adjusted**	
Midpoint (km)	**N**	**Eq. 3/ Radar**	**bias (m)**	**Adj./Radar**	**bias (m)**	**Adj./Radar**	**bias (m)**
1	146	0.97	-30	0.98	-20	1.00	0
2	209	0.99	-20	1.00	0	1.03	60
3	245	1.00	0	1.02	60	1.04	120
4	249	0.98	-80	1.00	0	1.02	80
5	234	0.95	-250	0.98	-100	0.99	-50
6	205	0.93	-420	0.96	-240	0.98	-120
7	136	0.91	-630	0.94	-420	0.96	-280
8	88	0.89	-880	0.92	-640	0.94	-480
All Distances	1512	0.95	-50	0.97	-30	1.00	0

Table 16. 95% confidence intervals (Eq. 4) for targets at the given distances, including bias. Target distances in the first column were multiplied by the ratios from Table 15 for each distance and method to calculate the mean around which the confidence interval was centered. Confidence intervals were calculated from: "Unadjusted" = Eq. *3*; "Refraction-adjusted" = reticle measurements adjusted for average refraction (with temperature gradient = -0.02); "Final" = adjusted both for refraction and ship-specific (Model 7) differences; "Measurement error" = ideal precision (no bias) based on simultaneous measurements to single targets.

Distance (km)	**Unadjusted s_2 = 0.1227 (Method # 31, Table 9)**		**Refraction-adjusted s_2 = 0.1150 (Method #19, Table 9)**		**Final s_2 = 0.1075 (Method #1, Table 9)**		**Measurement Error s_1 = 0.0719 (Equations 4, 5)**	
	lower 95%	**upper 95%**	**lower 95%**	**upper 95%**	**lower 95%**	**upper 95%**	**lower 95%**	**upper 95%**
1.0	0.8	1.2	0.8	1.2	0.8	1.2	0.9	1.2
2.0	1.6	2.5	1.6	2.5	1.7	2.5	1.7	2.3
3.0	2.4	3.8	2.4	3.8	2.5	3.9	2.6	3.5
4.0	3.1	5.0	3.2	5.0	3.3	5.0	3.5	4.6
5.0	3.7	6.1	3.9	6.1	4.0	6.1	4.3	5.8
6.0	4.4	7.1	4.6	7.2	4.8	7.3	5.2	6.9
7.0	5.0	8.1	5.2	8.2	5.4	8.3	6.1	8.1
8.0	5.6	9.0	5.8	9.2	6.1	9.3	6.9	9.2

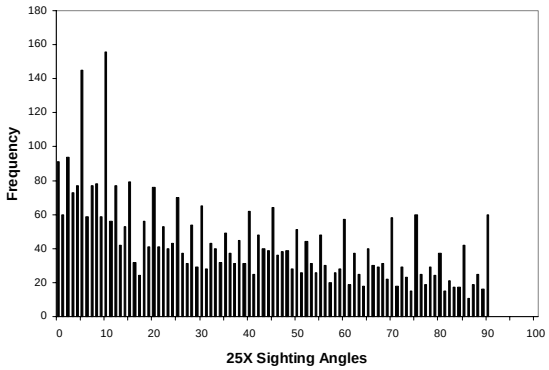

Figure 1a

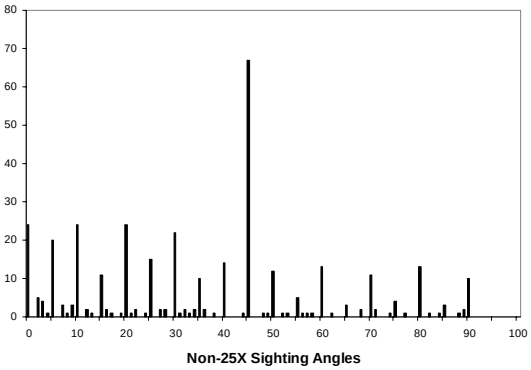

Figure 1b

Fig. 1. Horizontal sighting angles recorded during 1998-2000 line-transect surveys using: (a) angle rings at the base of 25X binoculars, and (b) non-25X sighting angles using unaided eye or 7X binoculars. Angles right or left of the trackline are combined in a single bin.

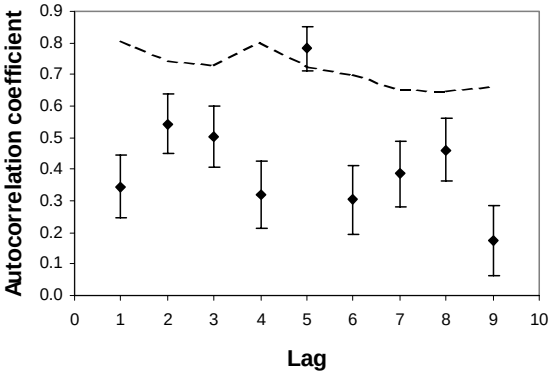

Figure 2a

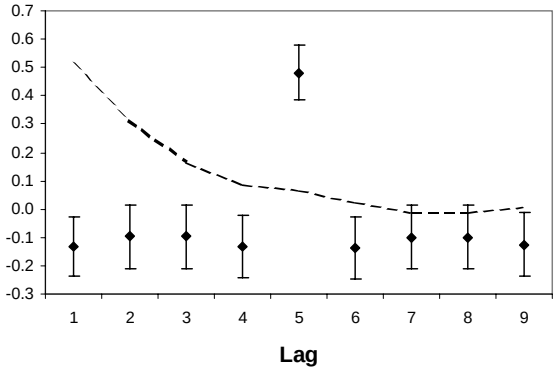

Figure 2b

Fig. 2. Autocorrelation coefficients for horizontal angle frequencies at 1 degree lags. Points with standard error bars indicate autocorrelation of original 25X measurements. Dotted lines connect measurements smeared over ±2 degrees ($\Delta\rho$ = 4, error bars not shown). 25X coefficients are reported in Table 3 and non-25X coefficients are from Table 4. Smeared values are averages of 20 runs. (a) original 25X angles (from Fig. 1a); and (b) non-25X angles (Fig. 1b).

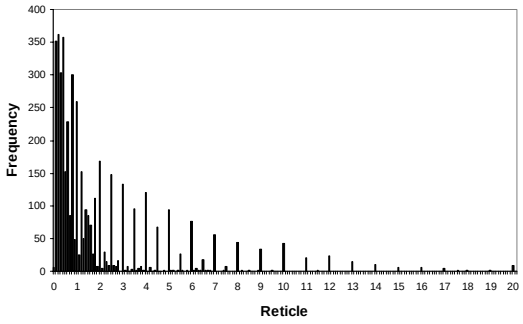

Figure 3a

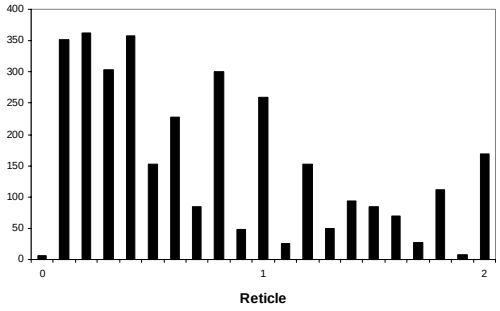

Figure 3b

Fig. 3. 25X reticle values recorded during 1998-2000 line-transect surveys in the eastern tropical Pacific ocean: (a) all reticles; (b) reticles ≤ 2.

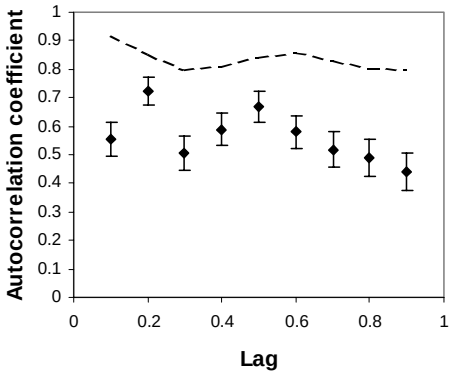

Figure 4a

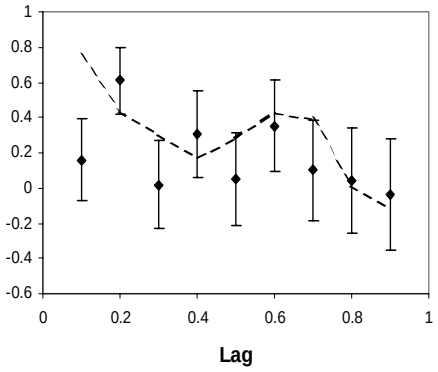

Figure 4b

Fig. 4. Autocorrelation coefficients for 25X reticles, lagged at 0.1 reticles. Points with standard error bars indicate autocorrelation of original reticle measurements. Dotted line connects reticle values smeared at ±0.05 reticles ($\Delta\rho = 0.1$). (a) all reticle values; and (b) reticles ≤ 2.

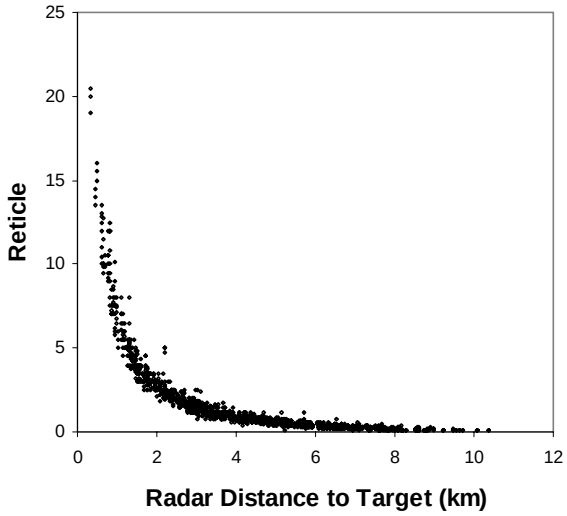

Fig. 5. Distribution of 25X binocular reticle values assigned by observers to targets versus the distances from radar to the targets.

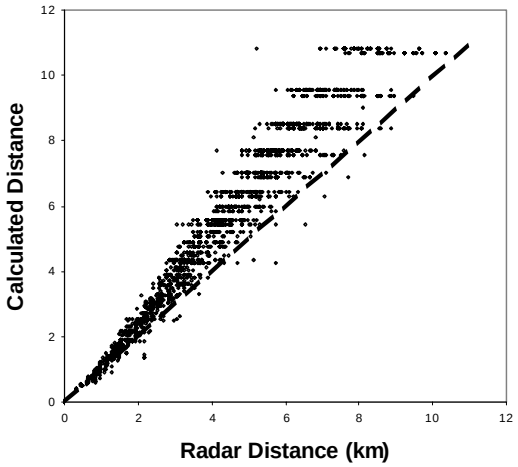

Fig. 6a

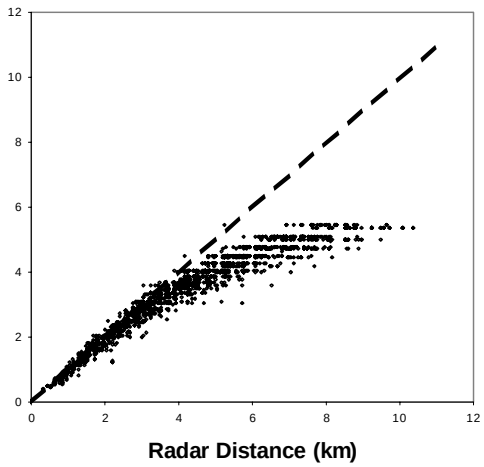

Fig. 6b

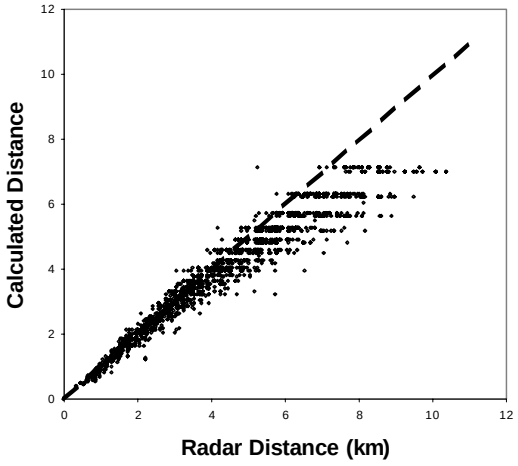

Fig. 6c

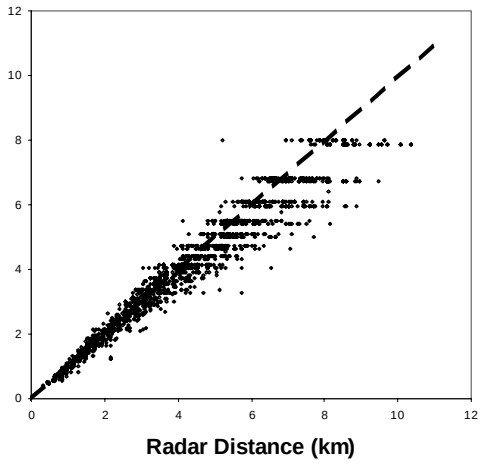

Fig. 6d

Fig. 6. Angle-to-distance conversion formulas from Table 3 applied to reticle values versus distances from radar. Dotted lines indicate 1:1 line for unbiased reticle estimates of distance. (a) Smith (1982); (b) Buckland et al. (1993); (c) Bowditch (1995); (d) Lerczak and Hobbs (1998) (Eq. *3*).

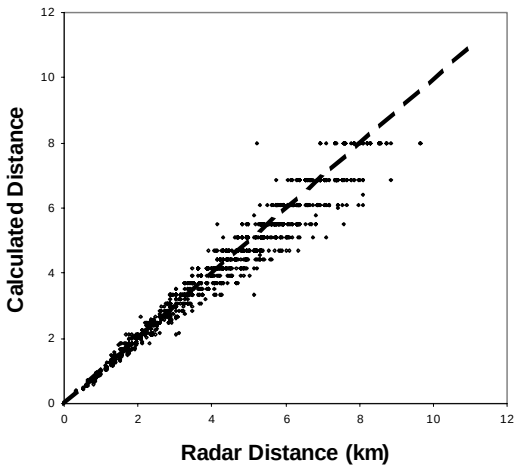

Fig. 7a

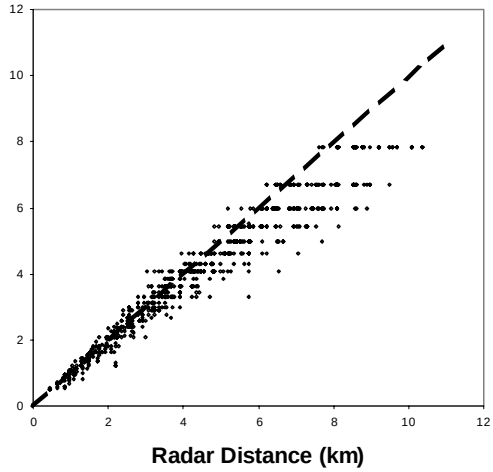

Fig. 7b

Fig. 7. Differences between ships in the fit of Eq. *3* distances to radar. (a) *Jordan*; (b) *McArthur*.

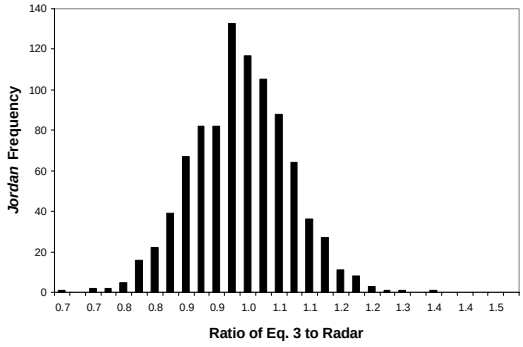

Fig. 8a

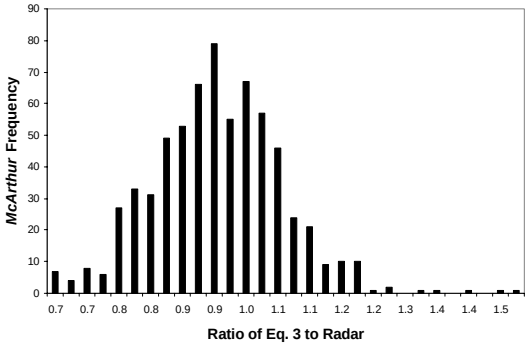

Fig. 8b

Fig. 8. Ratios of Eq. *3* distances to radar. (a) *Jordan* (b) *McArthur*.

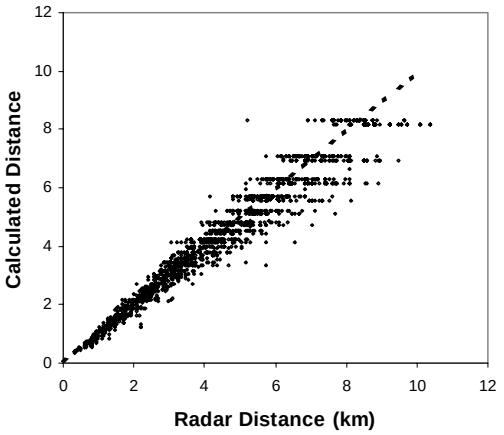

Fig. 9a

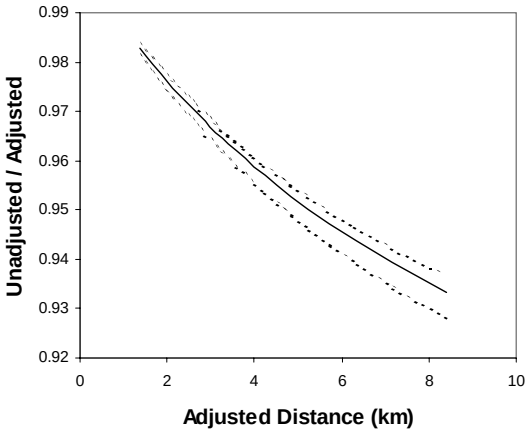

Fig. 9b

Fig. 9. Effect of adjusting reticle measurements for *local* refraction, and comparison of unadjusted to adjusted distance ratios of local *vs* average refraction. All calculations used the standard temperature gradient. (a) Distances adjusted based on local air temperatures and pressures in Eqs. *8-11* against distances from radar, both ships combined, and; (b) range of local refraction effects versus average refraction effects on the ratio of Eq. *3* distance to refraction-corrected distance. The lower dotted line indicates the unadjusted/adjusted ratio for the lowest air densities, produced from the combination of the highest measured air temperatures (32 deg) and lowest measured pressures (1008 mb); the upper dotted line indicates the ratio for the highest air densities, produced from the lowest temperatures (15 deg) and highest pressures (10019 mb); and the solid line indicates the ratio using average temperatures (25 deg) and pressures (1012 mb).

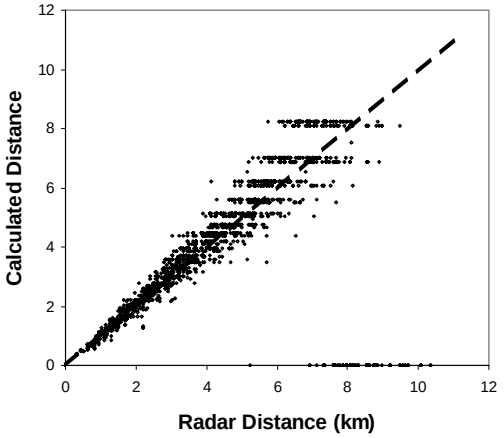

Fig. 10a

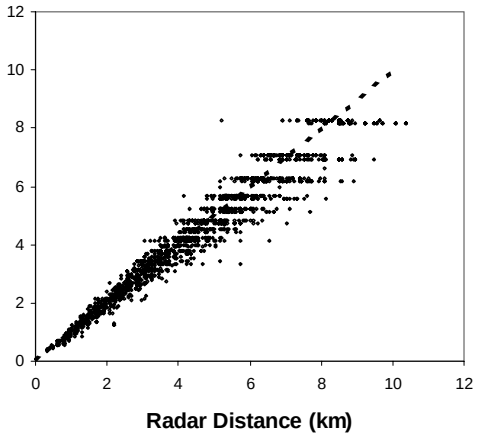

Fig. 10b

Fig. 10. (a) Distances obtained by replacing α in Eq. *3* with α_B from Eq. *7* (Bowditch 1995). Points lying along the x-axis at about 7-10 km represent reticle values of 0.1, which were undefined using this method. (b) Distances adjusted for refraction using *average* air temperatures and pressures and standard temperature gradient.

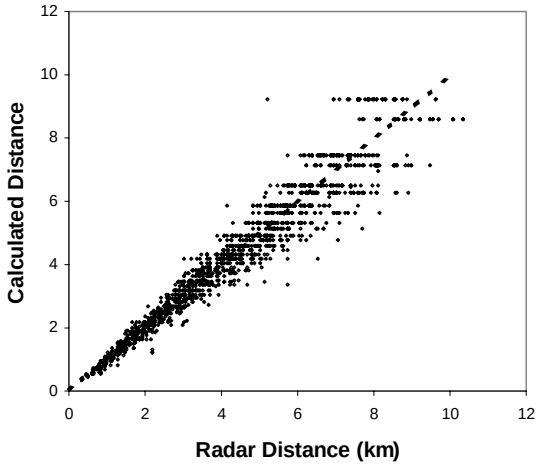

Fig. 11. Corrected distances against distances from radar using $\alpha_* = 0.00175$ for both ships in Eq. *3*. *Jordan* values (every other horizontal line of points starting with the top line) tend to be overcorrected, while the *McArthur* values (starting with the second line from the top) remain undercorrected.

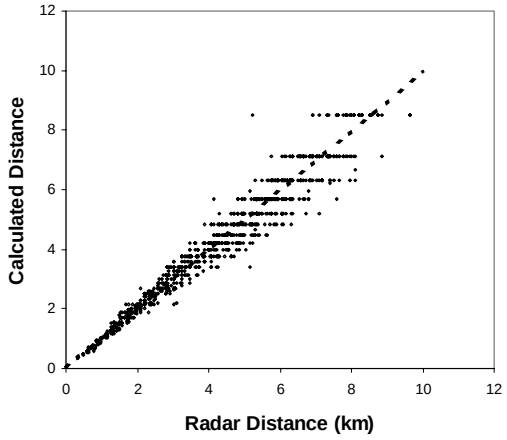

Fig. 12a

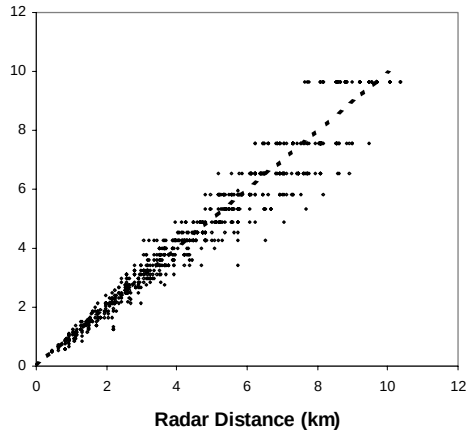

Fig. 12b

Fig. 12. Distances from reticles using ship-specific α_* values in Eq. *3* versus radar. (a) *Jordan* with $\alpha_* = 0.00179$, and; (b) *McArthur* with $\alpha_* = 0.00170$.

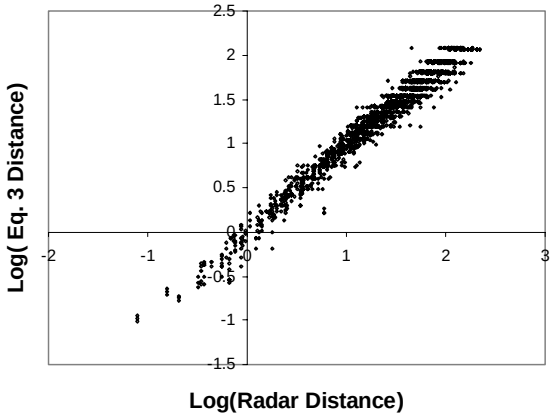

Fig. 13a

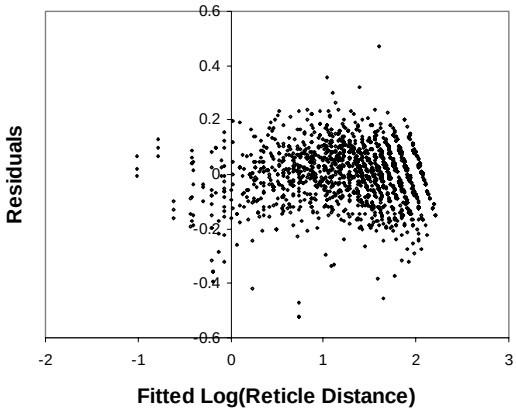

Fig. 13b

Fig. 13. (a) Logarithm of distance using Eq. *3* against logarithm of distance from radar. (b) Residuals from log-log regression (Eq. *12*) based on relationship in Fig. 13A.

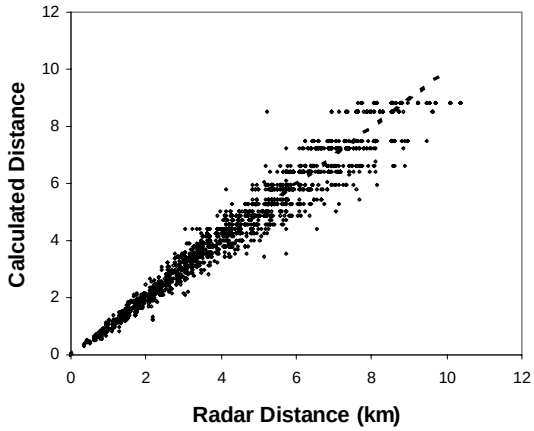

Fig. 14. 25X distances from reticles against distances from radar using non-explanatory regression-based correction method (Eq. *16*).

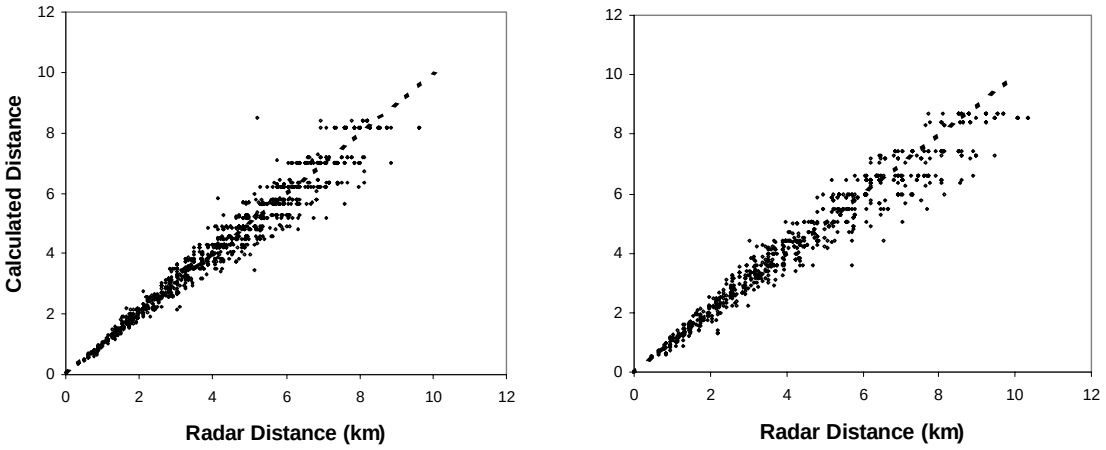

Fig. 15a Fig. 15b

Fig. 15. Distance from reticles against distance from radar for the final regression model (Eq. *18*), using refraction-corrected (average air temperature and pressure, fitted temperature gradient) distances. (a) *Jordan* (b) *McArthur*.

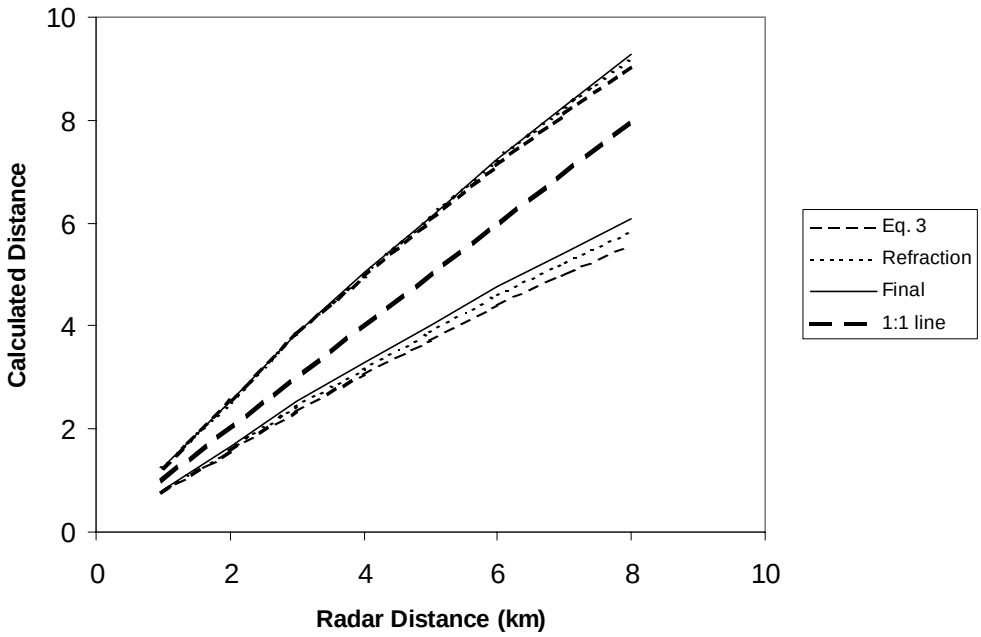

Fig. 16. 95% confidence intervals from Table 16 for measurements of distance using reticles. The dotted 1:1 line shows indicates exact measurement without variance or bias. Accuracy and precision of distance measurements using reticles under field conditions are shown for unadjusted Eq. *3*, refraction-only adjustment, and the final refraction + Model 7 adjustment.

Appendix A. Responses to comments by reviewers from the Center for Independent Experts.

On October 15-17, 2001, two reviewers from the Center for Independent Experts, Drs R. Mohn and P. Medley, read and made comments on an earlier version of this manuscript. Both agreed that the methods were sound and should improve the accuracy of perpendicular distances. Medley in addition expressed general support for corrections based on well-known physical effects (such as refraction) over regression-based adjustments to the distance measurements, but also expressed some concern that the data used for the refraction corrections were not available for all years. Following these reviews, we further developed the methodology of adjusting for refraction effects based on average temperatures and pressures and the fitted temperature gradient for the eastern tropical Pacific region. This enabled us to adjust all measurements in all years for the refraction component of the slight underestimate of distance using reticles. These developments were incorporated into the final estimates as described in this paper.